AGN Emission Models

Multiwavelength Variability and Polarization as Diagnostics of Jet Physics

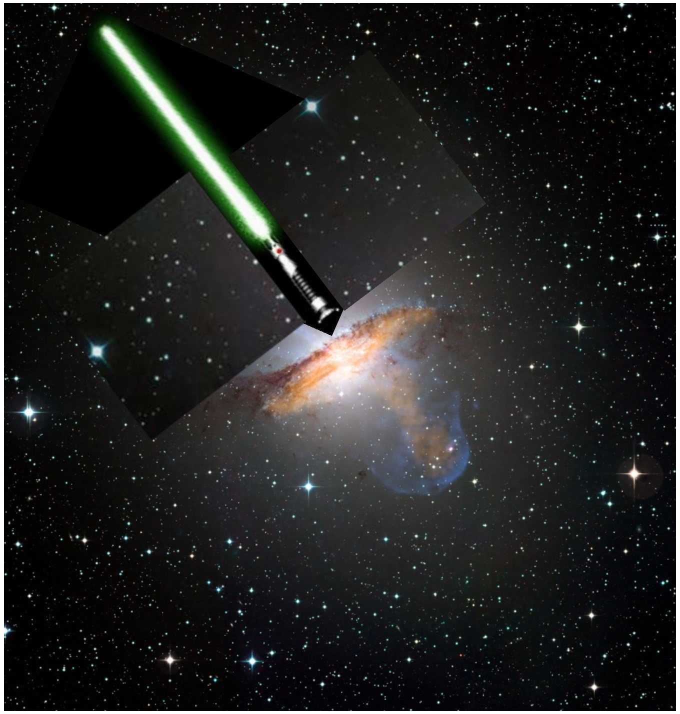

Markus Böttcher

North-West University

Potchefstroom

South Africa

NORTH-WEST UNIVERSITY®
YUNIBESITI YA BOKONE-BOPHIRIMA
NOORDWES-UNIVERSITEIT

Blazars

- Class of AGN consisting of BL Lac objects and gamma-ray bright quasars
- Rapidly (often intra-day) variable

- Strong gamma-ray sources
- Radio and optical polarization

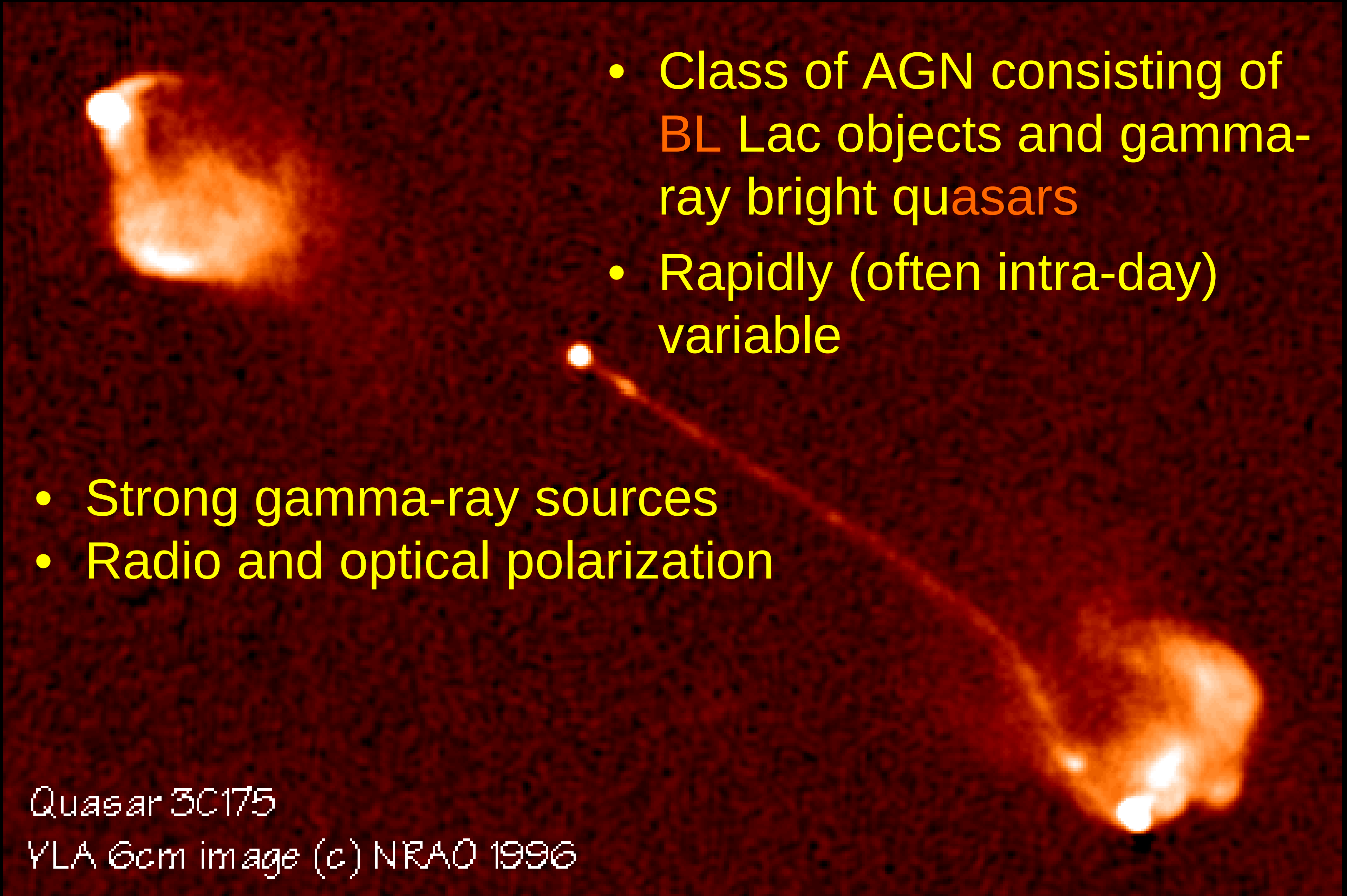

Polarization Angle Swings

- Optical + γ-ray variability of LSP blazars often correlated
- Sometimes O/γ flares correlated with increase in optical polarization and multiple rotations of the polarization angle (PA)

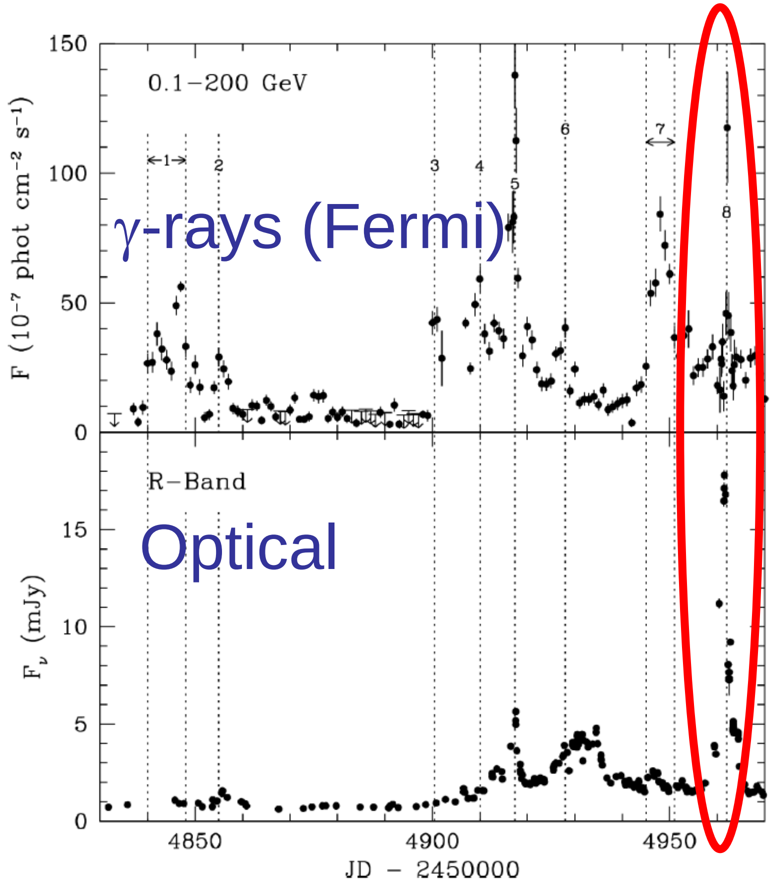

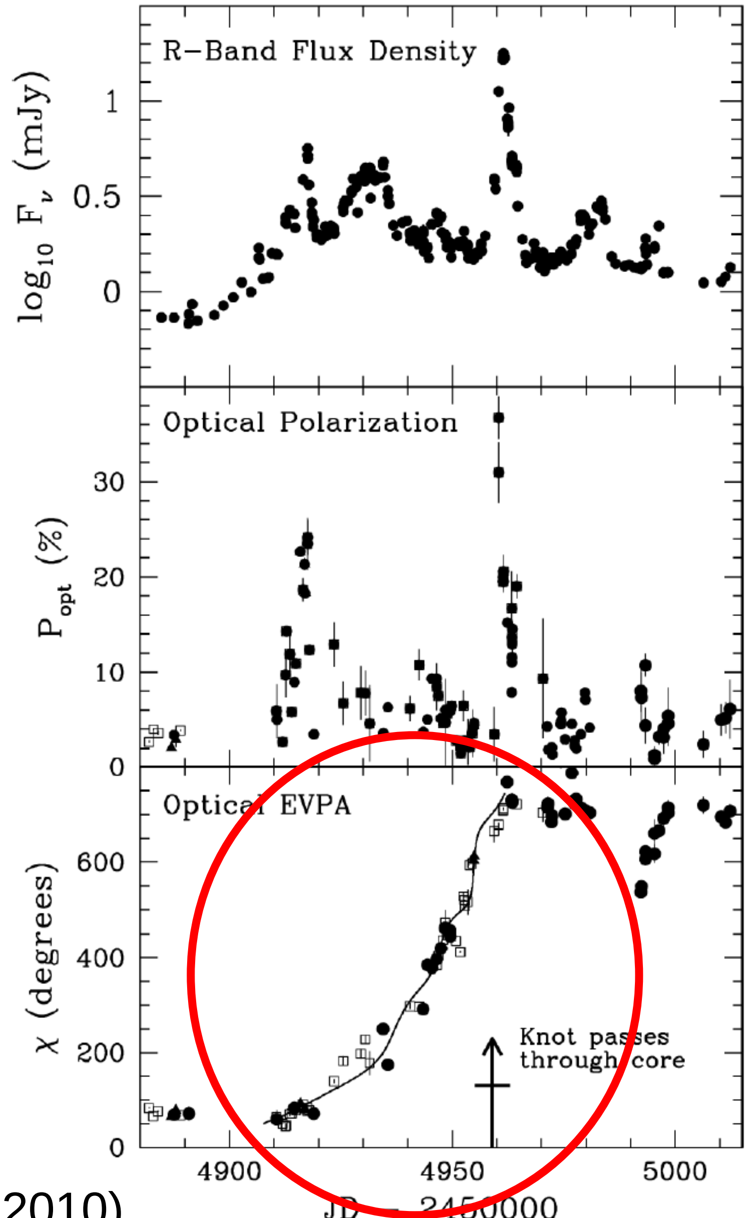

PKS 1510-089 (Marscher et al. 2010)

Blazars

- Class of AGN consisting of BL Lac objects and gamma-ray bright quasars
- Rapidly (often intra-day) variable

- Strong gamma-ray sources
- Radio and optical polarization
- Radio jets, often with superluminal motion

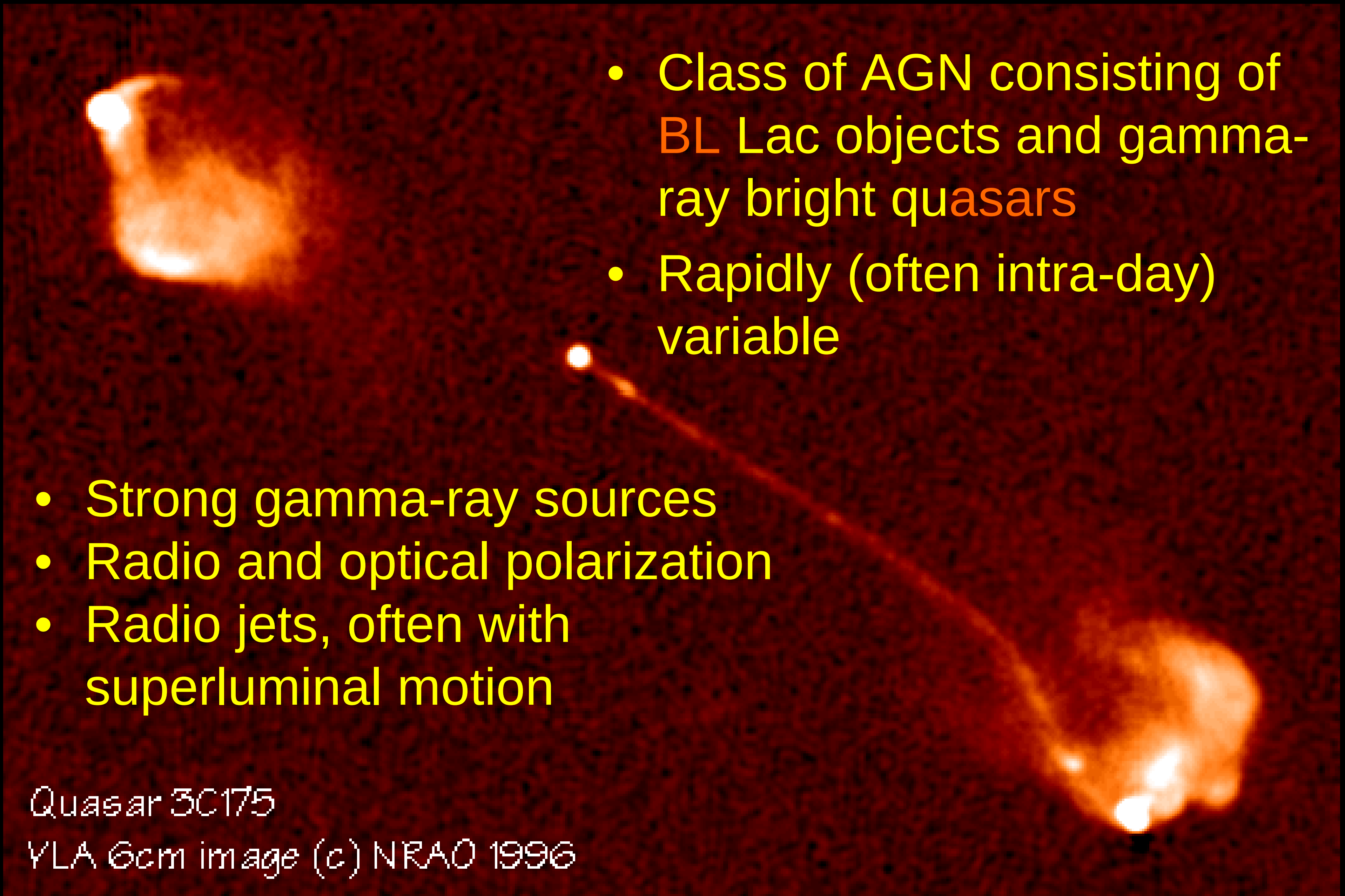

Open Physics Questions

- Source of Jet Power (Blandford-Znajek / Blandford/Payne?)
- Physics of jet launching / collimation / acceleration – role / topology of magnetic fields
- Composition of jets (e^--p or e^+-e^- plasma?) – leptonic or hadronic high-energy emission?
- Mode of particle acceleration (shocks / shear layers / magnetic reconnection?) – role of B fields
- Location of the energy dissipation / gamma-ray emission region

Leptonic Blazar Model

Injection, acceleration of ultrarelativistic electrons

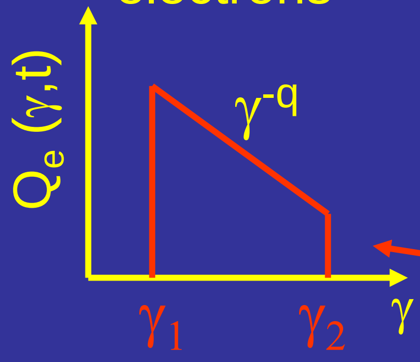

Relativistic jet outflow with $\Gamma \approx 10$

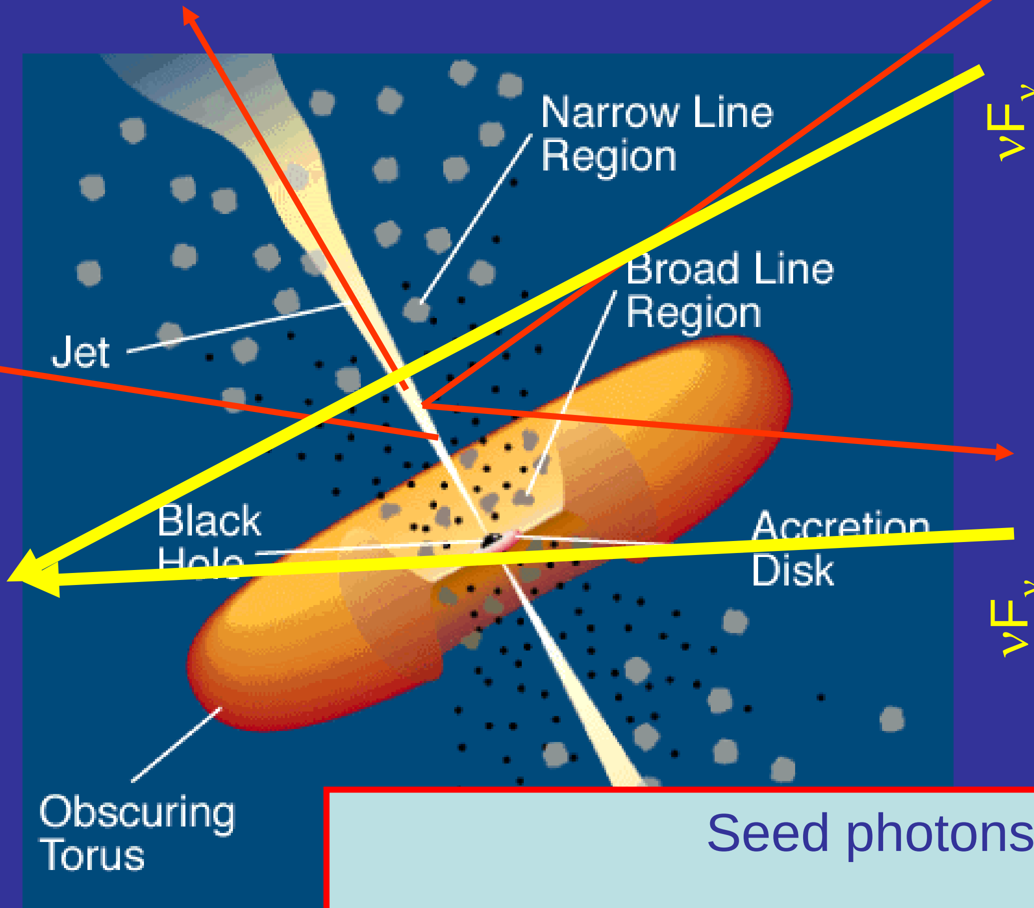

Synchrotron emission

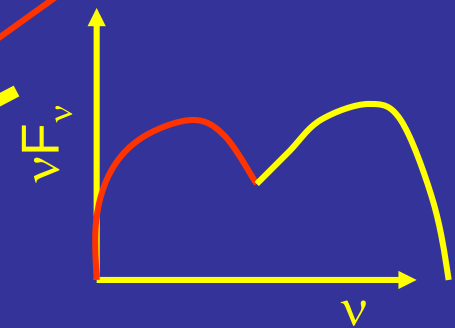

Compton emission

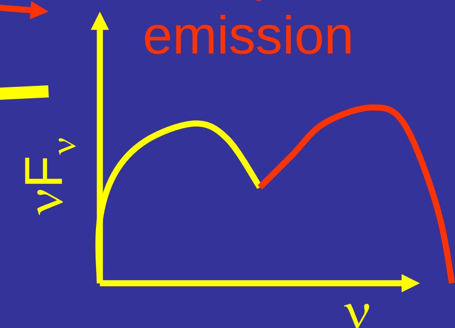

Radiative cooling ↔ escape =>

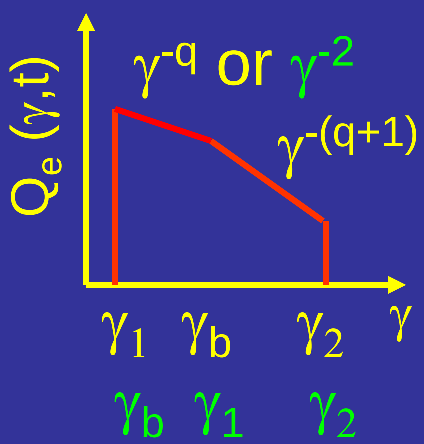

γ_b:
$\tau_{cool}(\gamma_b) = \tau_{esc}$

Seed photons:

Synchrotron (within same region [SSC] or slower/faster earlier/later emission regions [decel. jet]), Accr. Disk, BLR, dust torus (EC)

Sources of External Photons (↔ Location of the Blazar Zone)

Direct accretion disk emission (Dermer et al. 1992, Dermer & Schlickeiser 1994)
→ d < few 100 – 1000 R_s

Optical-UV Emission from the BLR (Sikora et al. 1994)
→ d < ~ pc

Infrared Radiation from the Obscuring Torus (Blazejowski et al. 2000)
→ d ~ 1 – 10s of pc

Synchrotron emission from slower/faster regions of the jet (Georganopoulos & Kazanas 2003)
→ d ~ pc - kpc

Spine – Sheath Interaction (Ghisellini & Tavecchio 2008)

→ d ~ pc - kpc

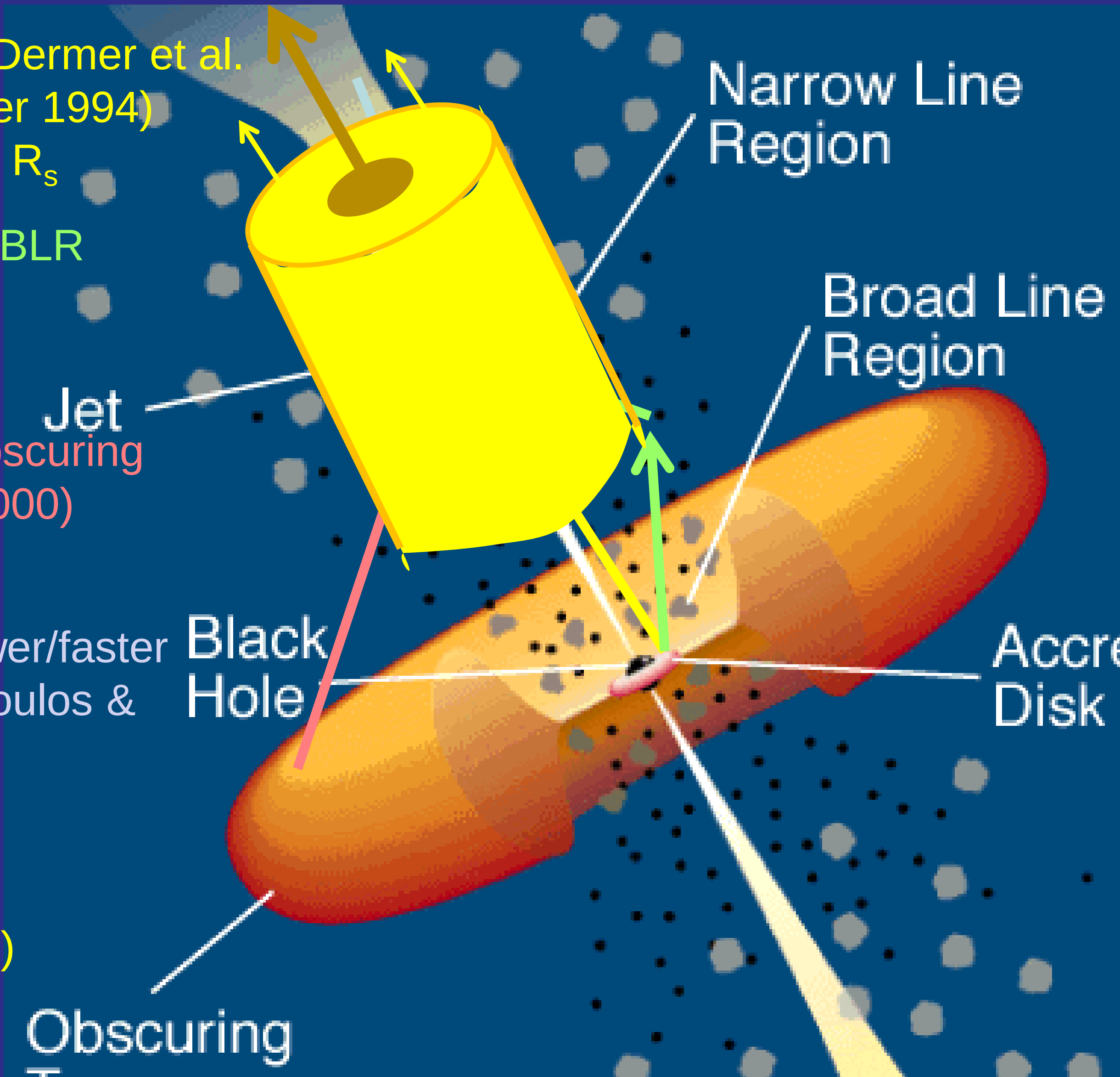

Hadronic Blazar Models

Injection, acceleration of ultrarelativistic electrons and protons

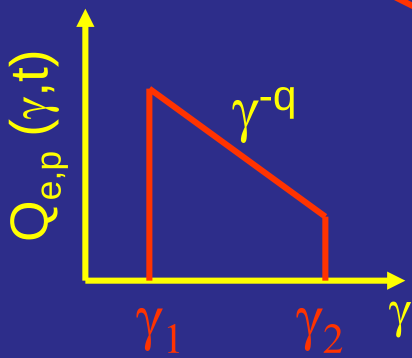

Relativistic jet outflow with $\Gamma \approx 10$

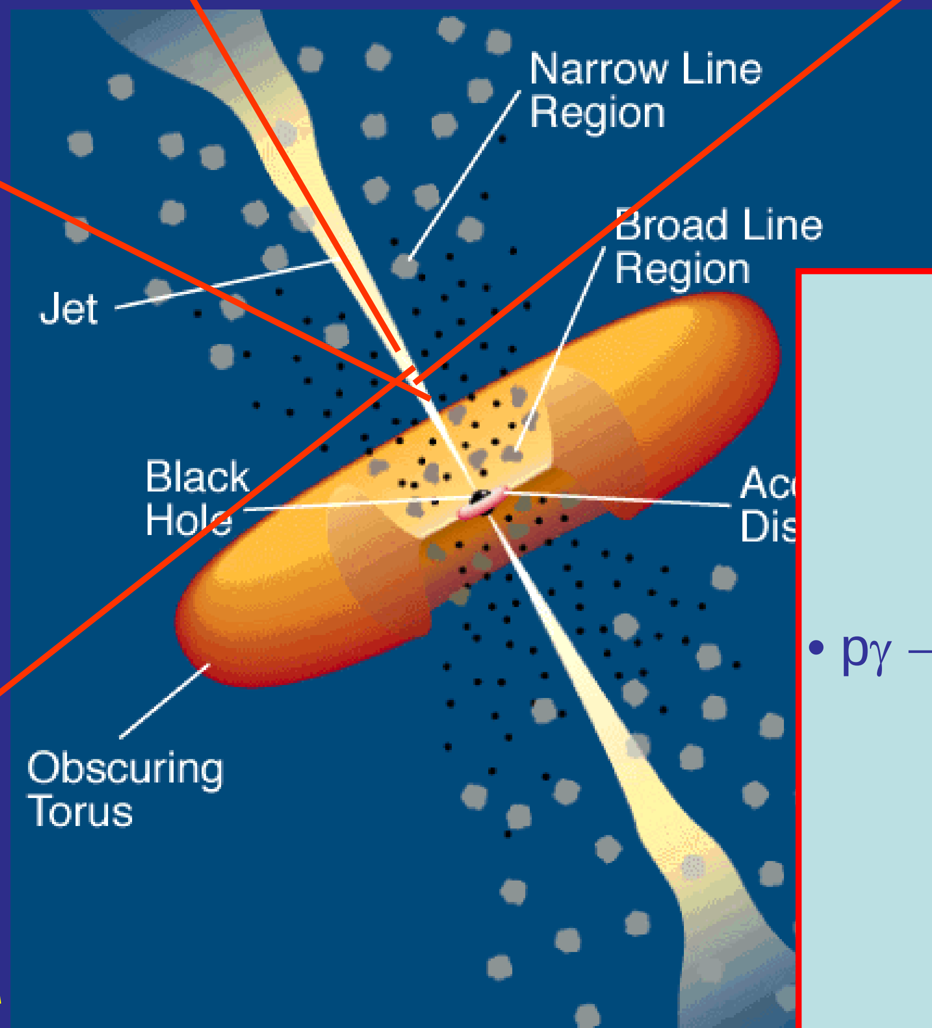

Proton-induced radiation mechanisms

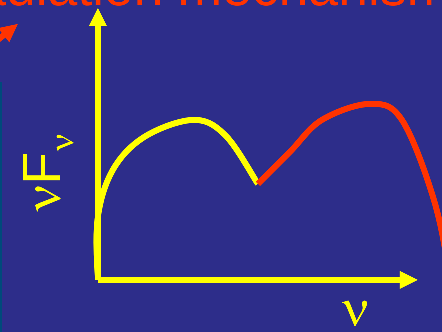

Synchrotron emission of primary e^-

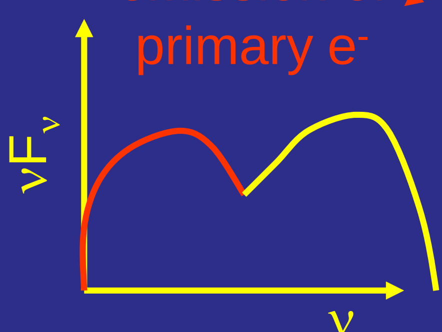

- Proton synchrotron
- $p\gamma \rightarrow p\pi^0$
  $\pi^0 \rightarrow 2\gamma$
- $p\gamma \rightarrow n\pi^+ ; \quad \pi^+ \rightarrow \mu^+\nu_\mu$
  $\mu^+ \rightarrow e^+\nu_e\overline{\nu_\mu}$
  $\rightarrow$ secondary μ-, e-synchrotron
- Cascades …

Gamma-Gamma Absorption

- External: EBL (Dominguez, Biteau, Gabici, …)
- Internal: BLR Radiation field

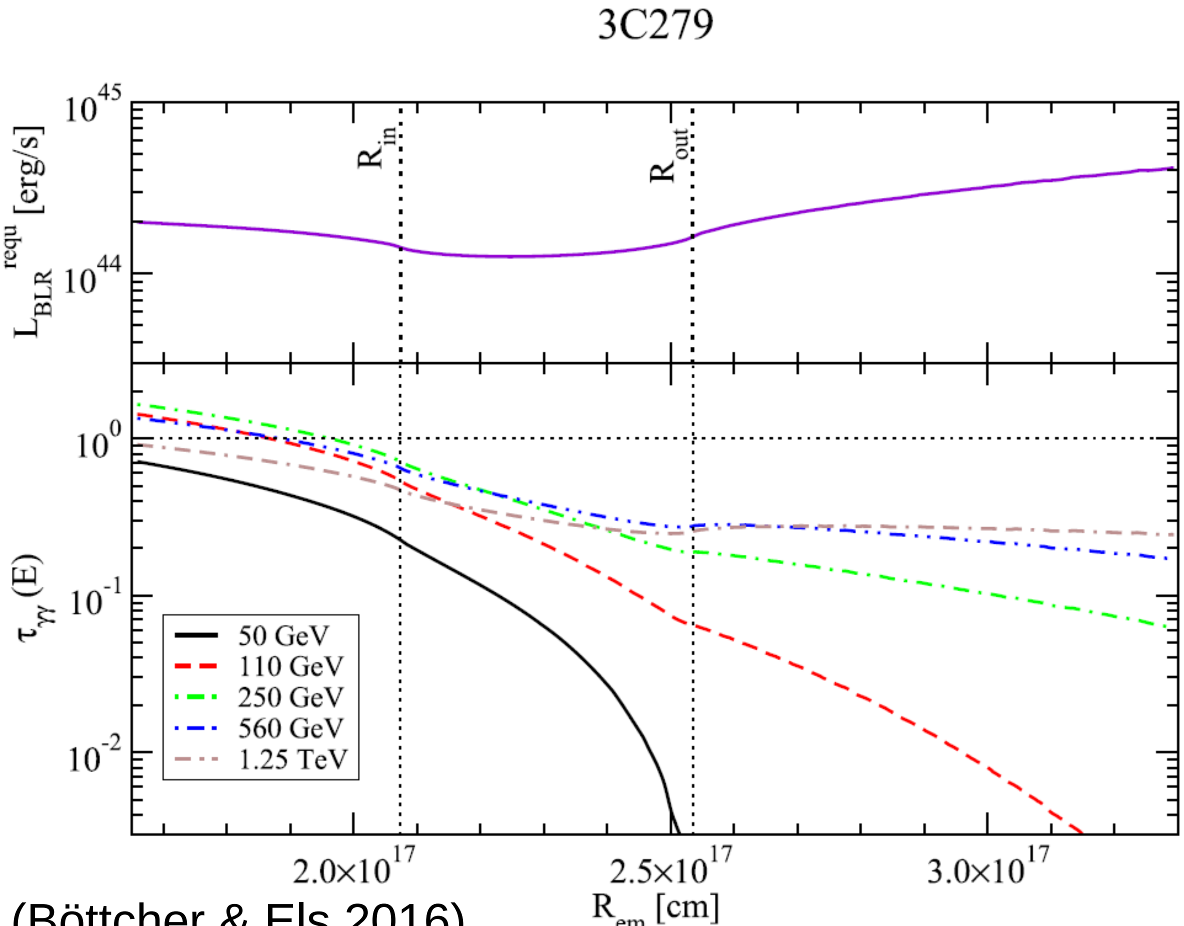

(Böttcher & Els 2016)

$R_{em} \geq R_{BLR}$

Constraint particularly important for VHE-detected FSRQs (3C279, PKS 1510-089, …)

Leptonic and Hadronic Model Fits along the Blazar Sequence

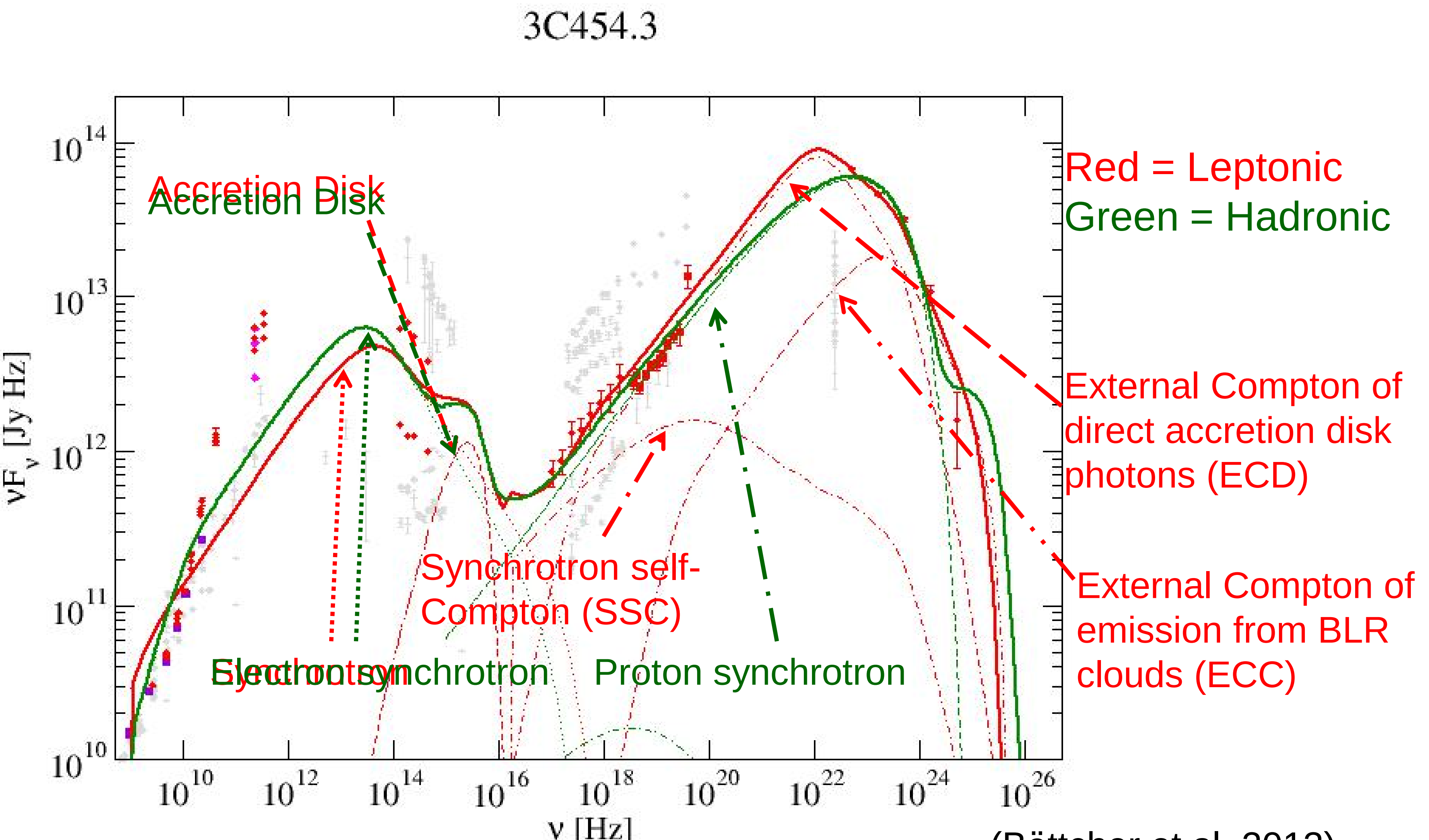

(Böttcher et al. 2013)

Leptonic and Hadronic Model Fits Along the Blazar Sequence

3C66A (IBL)

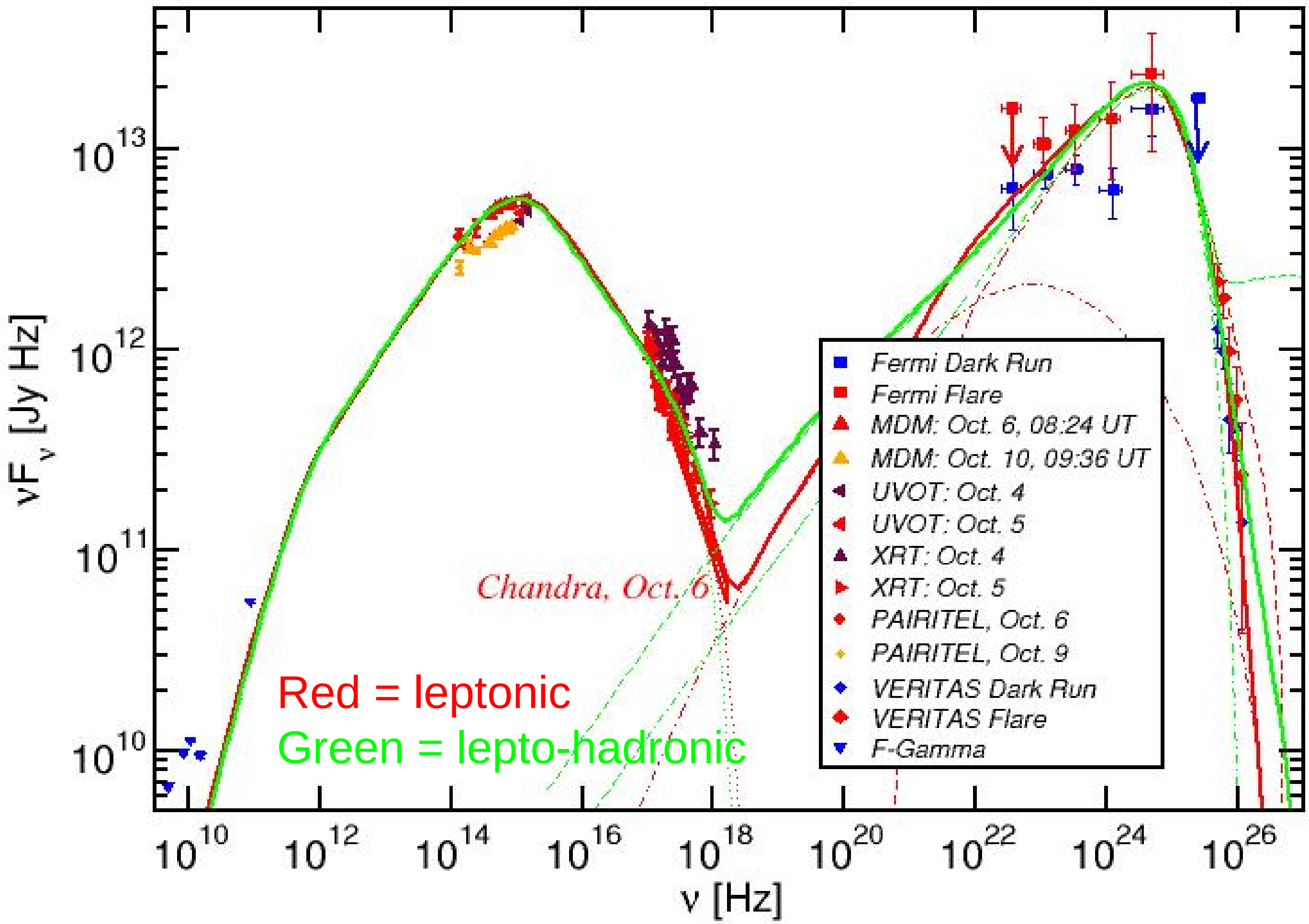

Lepto-Hadronic Model Fits Along the Blazar Sequence

RGB J0710+591 (HBL)

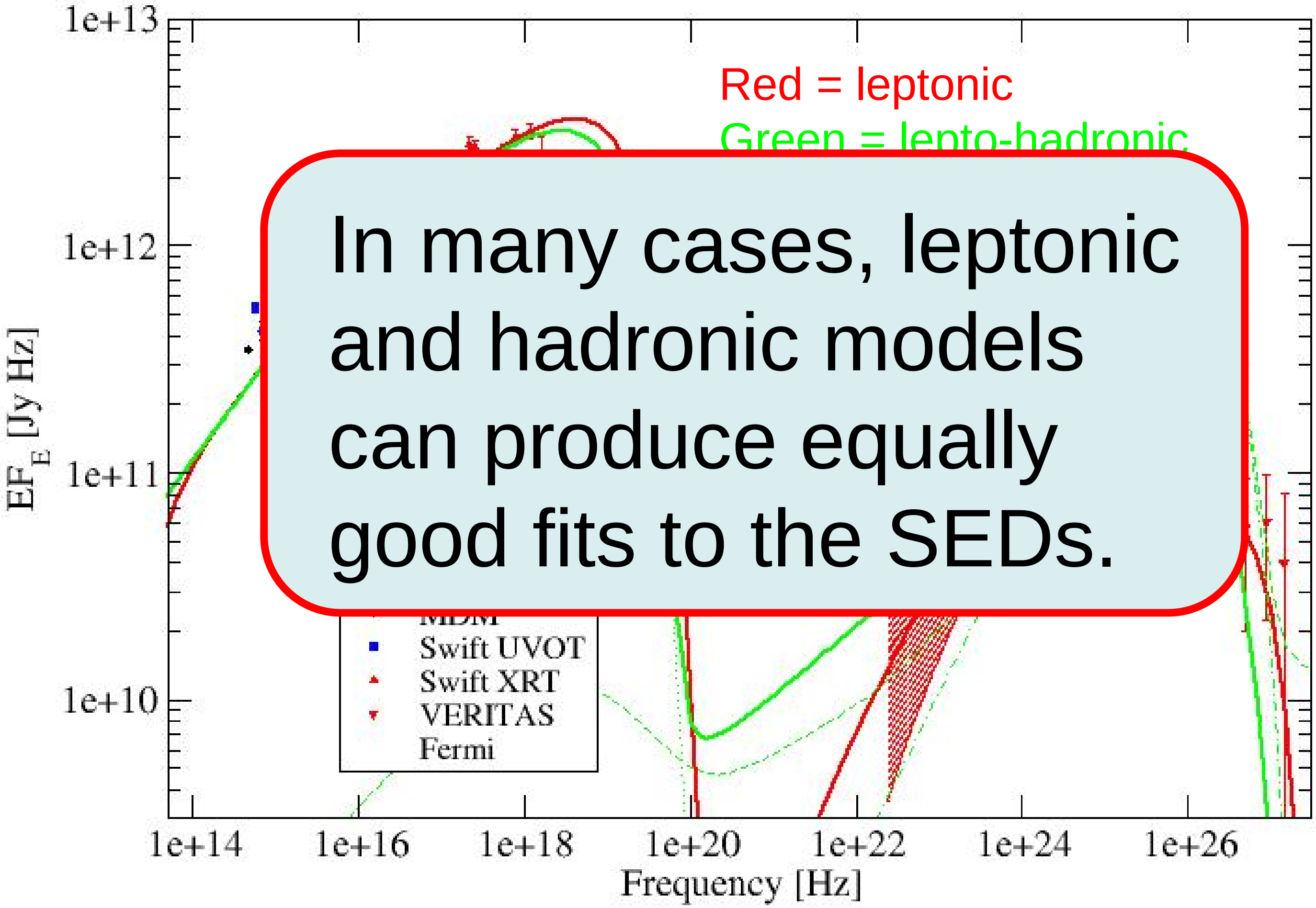

In many cases, leptonic and hadronic models can produce equally good fits to the SEDs.

Possible Diagnostics to distinguish:

- Neutrinos
- Variability
- Polarization

Requirements for lepto-hadronic models

- To exceed p-γ pion production threshold on interactions with synchrotron (optical) photons: $E_p > 7\times10^{16}\ E^{-1}_{ph,eV}$ eV
- For proton synchrotron emission at multi-GeV energies: E_p up to ~ 10^{19} eV (=> UHECR)
- Require Larmor radius

  $r_L \sim 3\times10^{16}\ E_{19}/B_G$ cm $\leq$ a few x 10^{15} cm => $B \geq 10$ G

  (Also: to suppress leptonic SSC component below synchrotron) – inconsistent with radio-core-shift measurements if emission region is located at ~ pc scales (e.g., Zdziarski & Boettcher 2015).
- Low radiative efficiency: Requiring jet powers $L_{jet} \sim L_{Edd}$

Distinguishing Diagnostic: Variability

In homogeneous, single-zone (spherical-cow) models:

- Time-dependent evolution of particle spectra:

$$\frac{\partial n_i(\gamma,t)}{\partial t} = \frac{\partial}{\partial \gamma}\left[\frac{\gamma^2}{(a+2)t_{\rm acc}}\frac{\partial n_i(\gamma,t)}{\partial \gamma}\right] - \frac{\partial}{\partial \gamma}(\dot{\gamma}\cdot n_i(\gamma,t)) + Q_i(\gamma,t) - \frac{n_i(\gamma,t)}{t_{\rm esc}} - \frac{n_i(\gamma,t)}{\gamma t_{\rm decay}}$$

Diffusion in momentum space (stochastic acceleration)

Systematic energy gain/loss (radiative losses)

"Injection" (pick-up, rapid acceleration, parent particle decay)

Escape

Decay (for unstable particles: n, $\pi^{\pm}$, $\mu^{\pm}$)

- And corresponding radiation transfer

- Variations of input parameters to model variability

(e.g., Mastichiadis & Kirk 1997; Li & Kusunose 2000; Böttcher & Chiang 2002; Chen et al. 2011; Diltz & Böttcher 2014; Diltz et al. 2015; …)

Distinguishing Diagnostic: Variability

3C454.3 Flare of November 2010

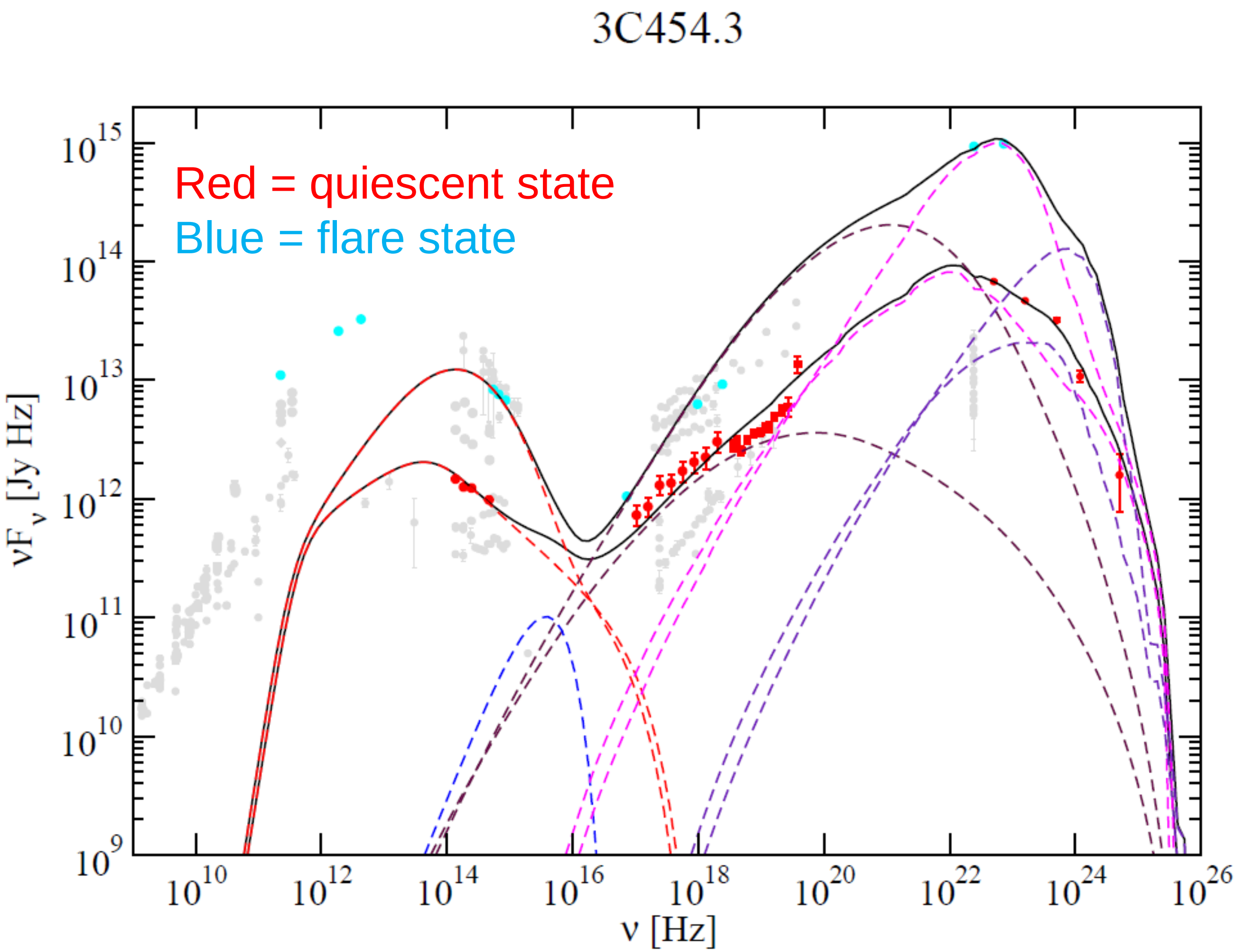

(Diltz & Böttcher 2016)

Time-dependent leptonic model

Best-fit variation of

- electron injection power
- B-field
- Stochastic acceleration time-scale

Poor fit to flare-state X-ray spectrum!

3C454.3 Flare of November 2010

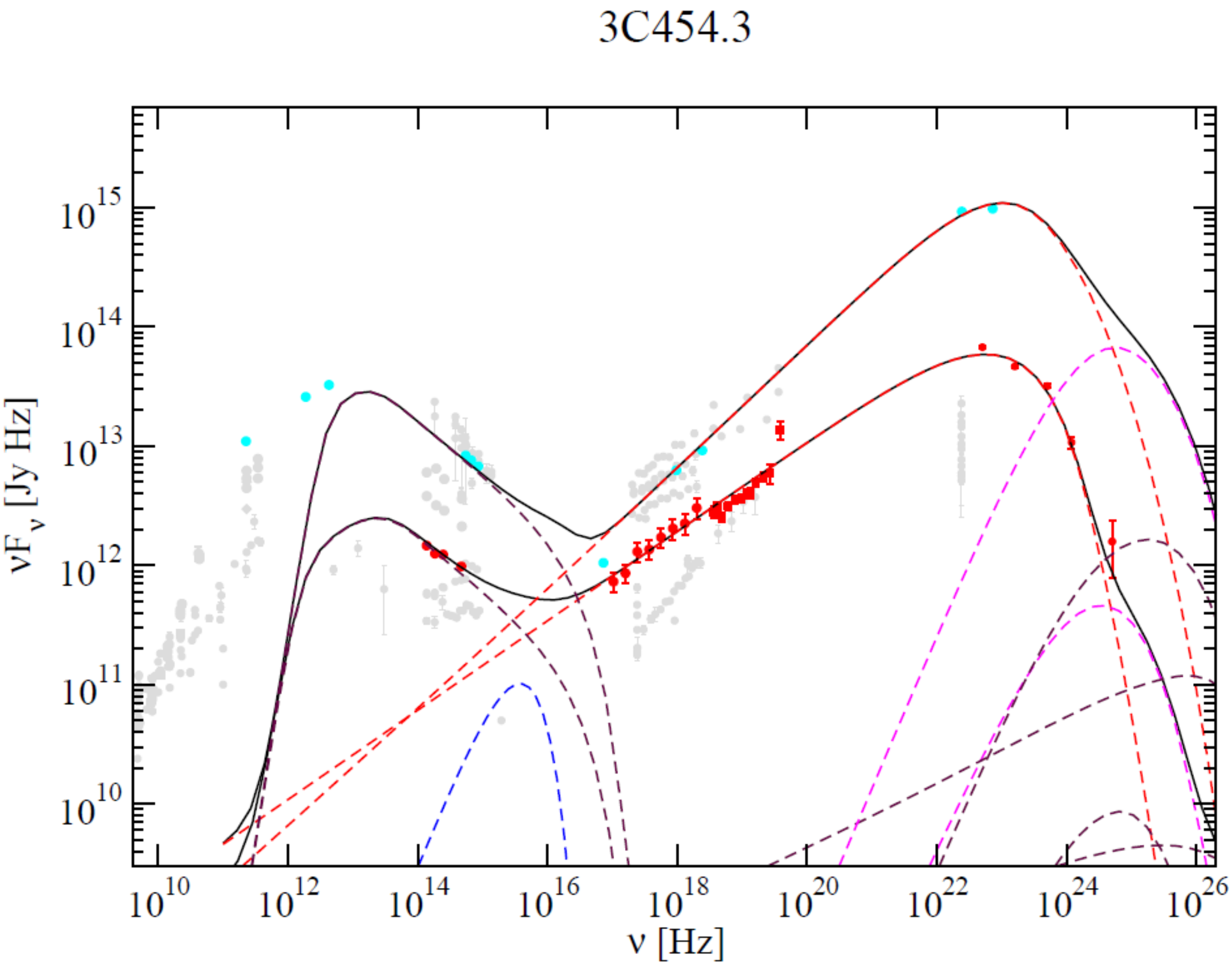

(Diltz & Böttcher 2016)

Time-dependent lepto-hadronic model

Best-fit variation of

- electron injection power
- B-field
- Stochastic acceleration time-scale
- Proton injection spectral index

Both quiescent and flare state well represented!

Light Curve Fits

3C454.3 Flare of November 2010

Red = lepto-hadronic
Green - leptonic

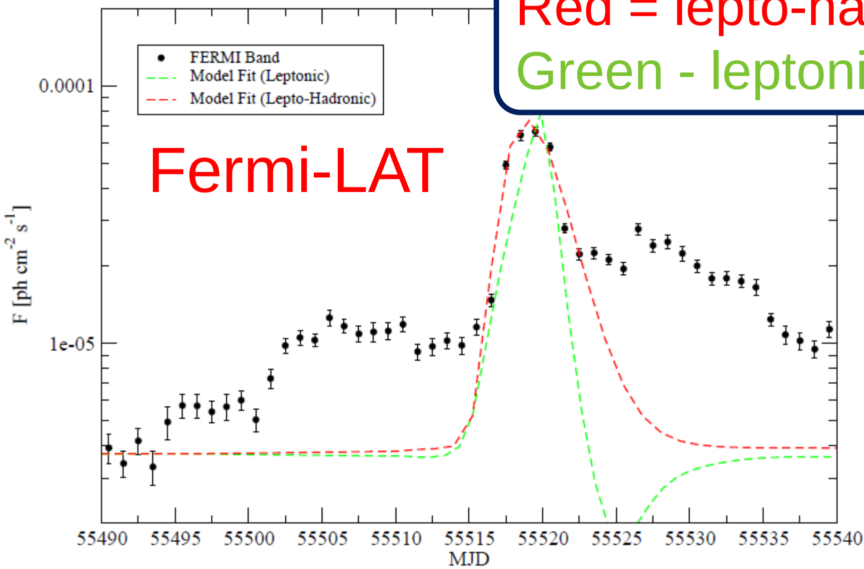

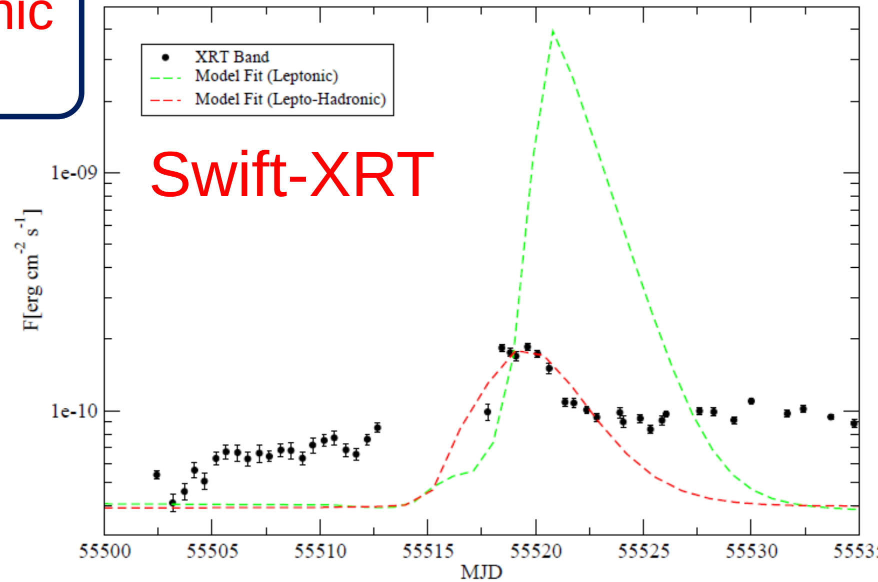

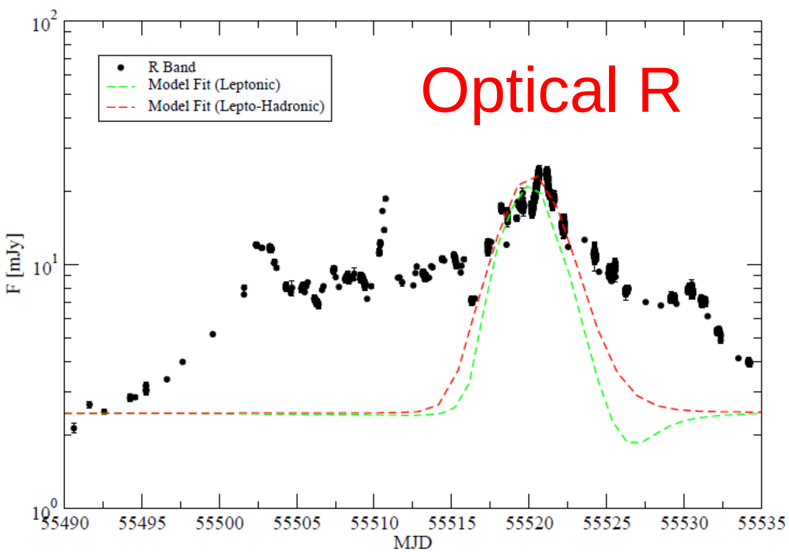

Good simultaneous fits to snap-shot SEDs **and** multiwavelength light curves with lepto-hadronic model (but requiring $L_p \sim L_{Edd}$!)

Poor fits to flaring-state X-ray spectrum **and** X-ray light curve with leptonic model.

(Diltz & Böttcher 2016)

Neutrino Emission

Most hadronic / lepto-hadronic models of blazars are proton-synchrotron dominated => Very low expected neutrino flux

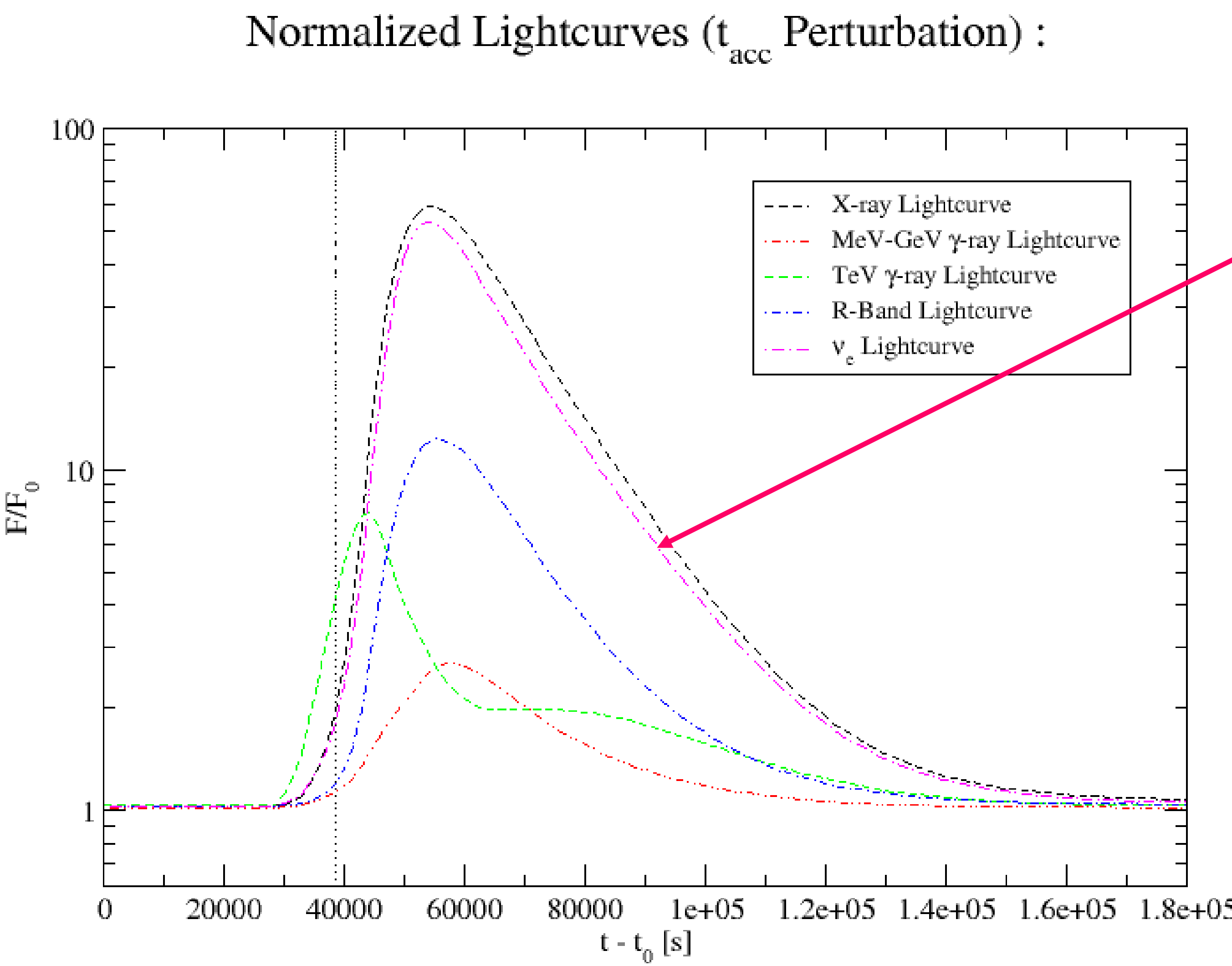

Neutrino flares generally co-incident with X-ray through GeV γ-ray flares:

IceCube detection rates:

- ~ 0.3 yr^{-1} (quiesc.)
- ~ 3 yr^{-1} (flares)

(Diltz et al. 2015)

Distinguishing Diagnostic: Polarization

- Synchrotron Polarization

For synchrotron radiation from a power-law distribution of electrons with ne $(\gamma) \sim \gamma^{-p}$ $\rightarrow$ $F_\nu \sim \nu^{-\alpha}$ with $\alpha = (p-1)/2$

$$\Pi^{sy}_{PL} = \frac{p+1}{p+7/3} = \frac{\alpha+1}{\alpha+5/3}$$

$p = 2 \rightarrow \Pi = 69\ \%$

$p = 3 \rightarrow \Pi = 75\ \%$

Compton Polarization

Compton cross section is polarization-dependent:

$$\frac{d\sigma}{d\Omega} = \frac{r_0^2}{4}\left(\frac{\epsilon'}{\epsilon}\right)^2\left(\frac{\epsilon}{\epsilon'} + \frac{\epsilon'}{\epsilon} - 2 + 4\left[\vec{e}\cdot\vec{e}'\right]^2\right)$$

$\varepsilon = h\nu/(m_e c^2)$:

Thomson regime: $\varepsilon \approx \varepsilon'$

$\Rightarrow d\sigma/d\Omega = 0$ if $\vec{e}\cdot\vec{e}' = 0$

$\Rightarrow$ Scattering preferentially in the plane perpendicular to $\vec{e}$!

Preferred polarization direction is preserved; polarization degree reduced to ~ ½ of target-photon polarization .

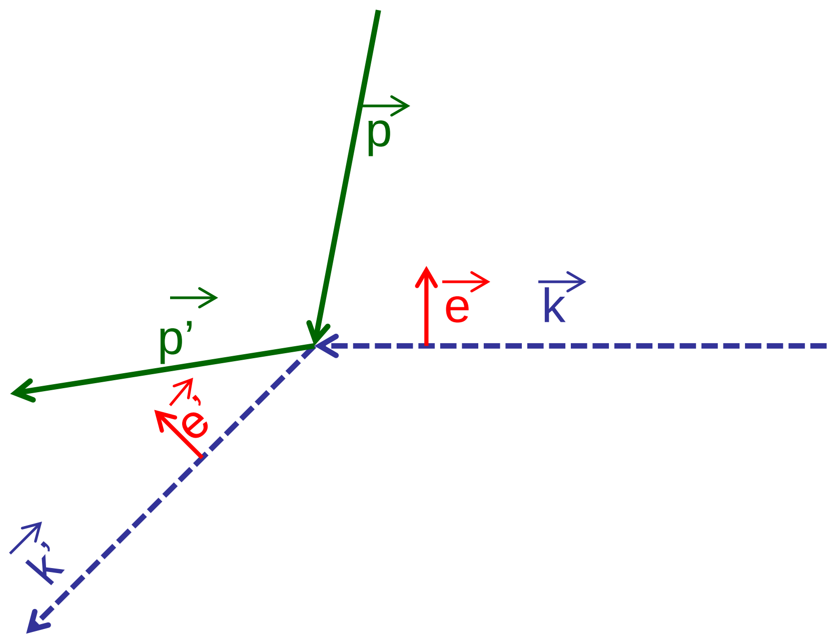

X-Ray and Gamma-Ray Polarization: FSRQs

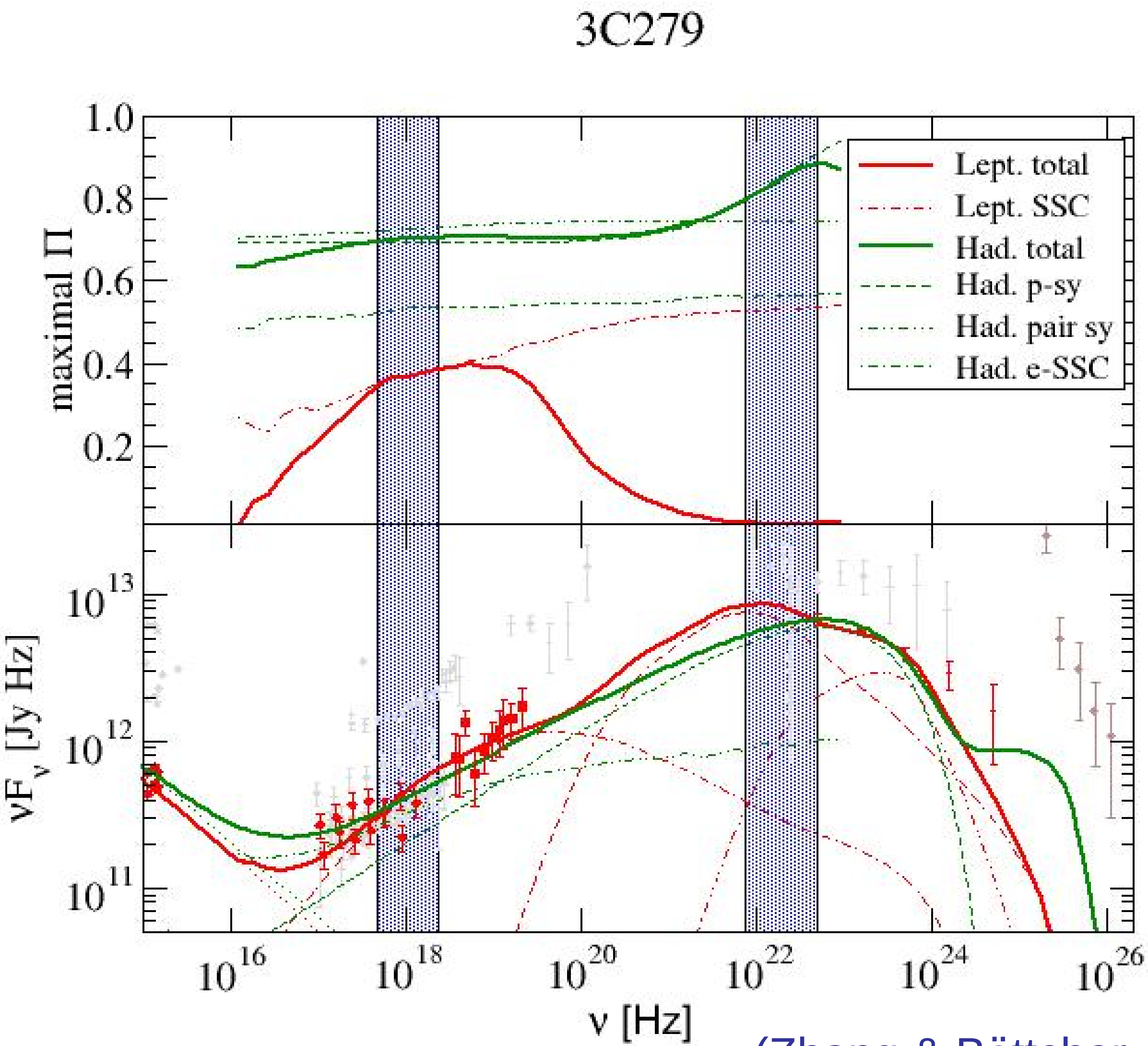

Hadronic model: Synchrotron dominated => High Π, generally increasing with energy (SSC contrib. in X-rays).

Leptonic model: X-rays SSC dominated: Π ~ 20 – 40 %; γ-rays EC dominated => Negligible Π.

(Zhang & Böttcher, 2013)

X-Ray and Gamma-Ray Polarization: IBLs

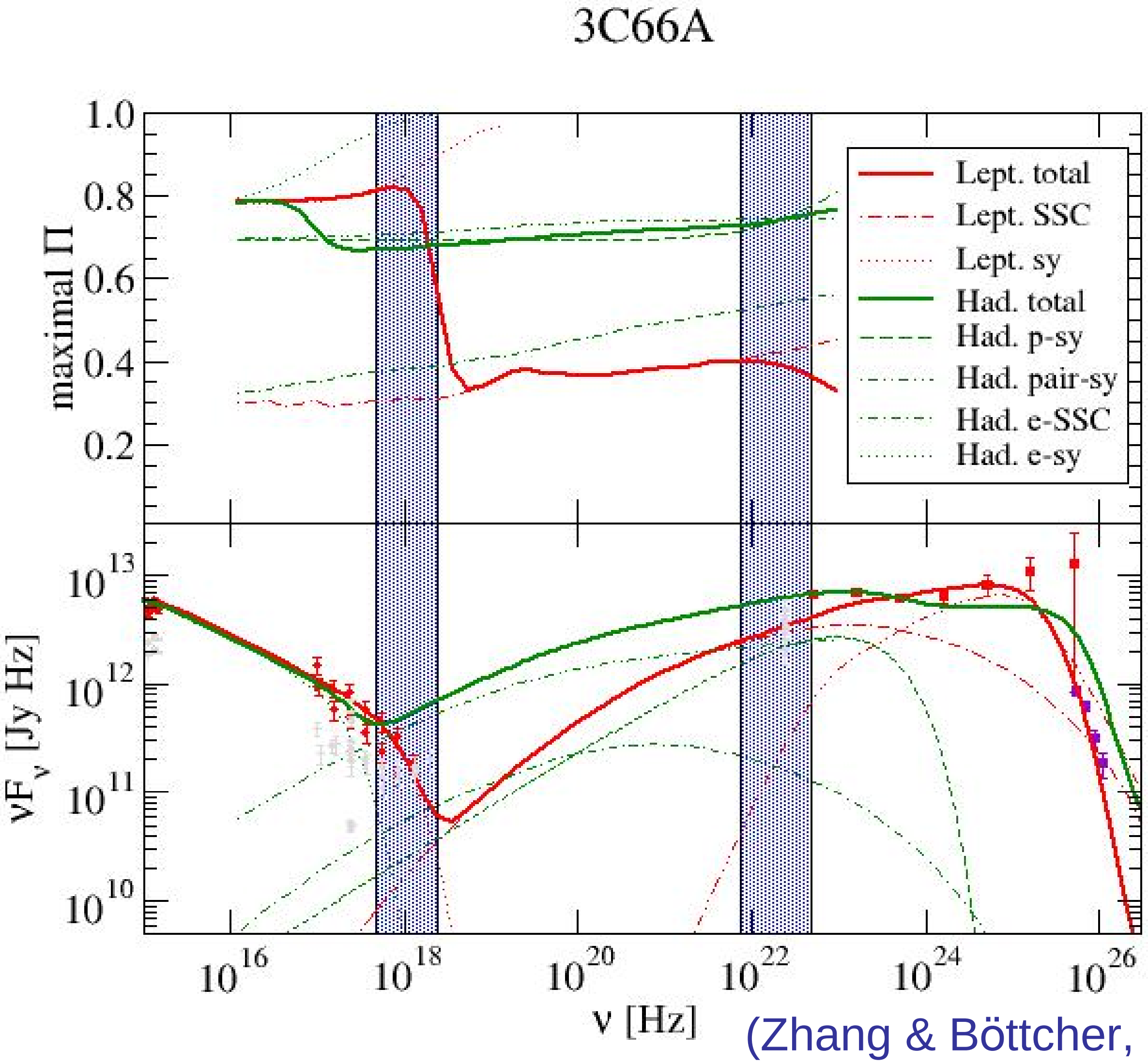

Hadronic model:
Synchrotron dominated => High Π, throughout X-rays and γ-rays

Leptonic model:
X-rays sy. Dominated => High Π, rapidly decreasing with energy; γ-rays SSC/EC dominated => Small Π.

(Zhang & Böttcher, 2013)

Observational Strategy

- Results shown here are **upper limits** (perfectly ordered magnetic field perpendicular to line of sight)

- Scale results to actual B-field configuration from known synchrotron polarization (e.g., optical for FSRQs/LBLs)
  => Expect 10 - 20 % X-ray and γ-ray polarization in hadronic models!

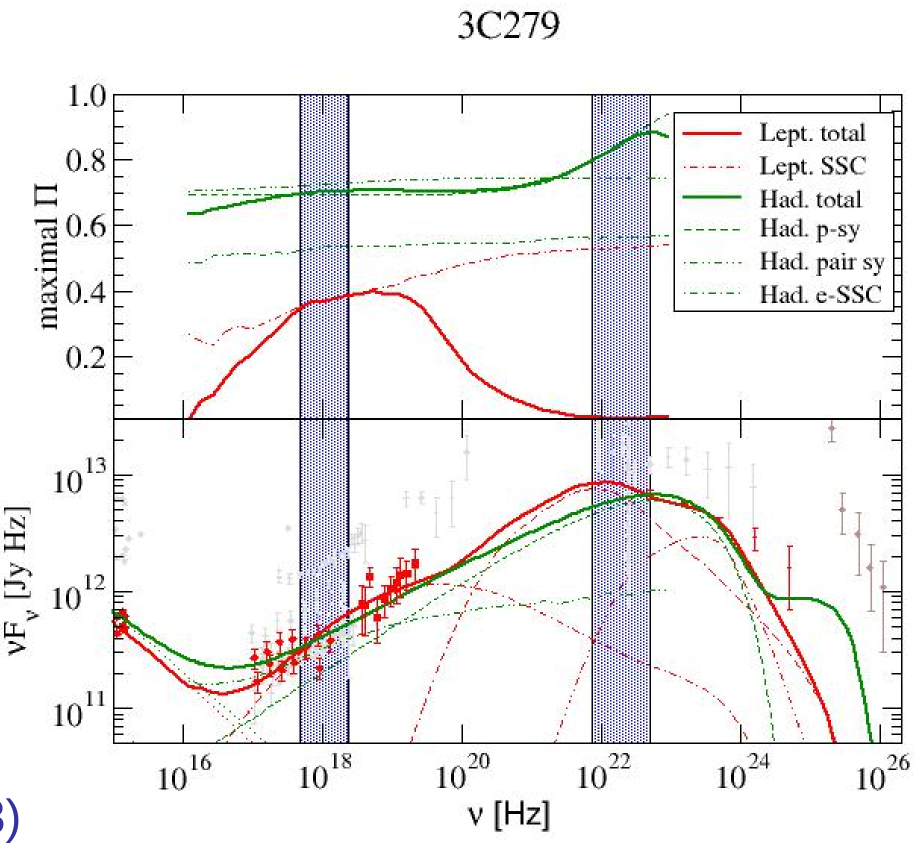

- X-ray and γ-ray polarization values substantially below synchrotron polarization will favor leptonic models, measurable γ-ray polarization clearly favors hadronic models!

(Zhang & Böttcher 2013)

So far, only Spherical-Cow Models

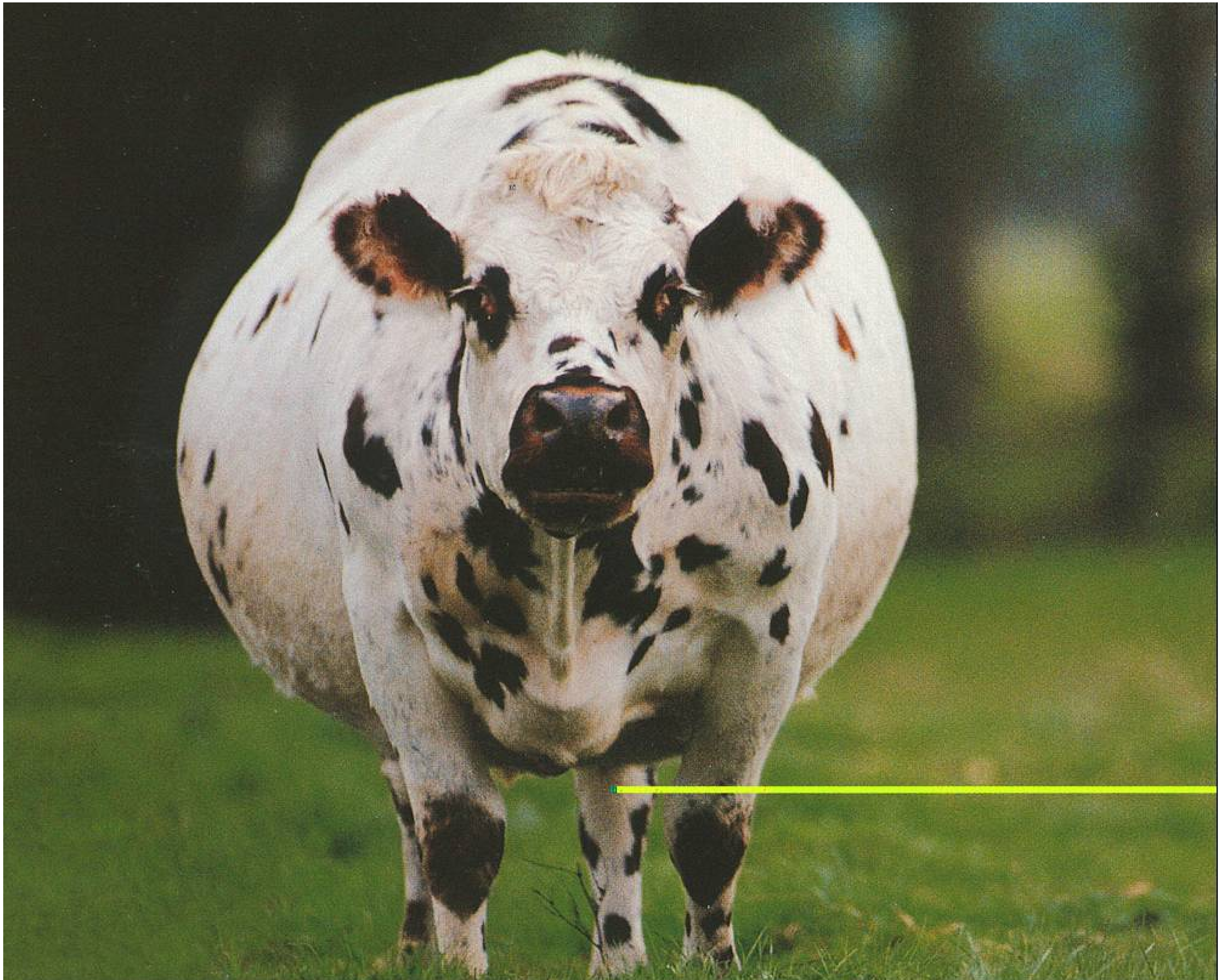

Inhomogeneous Jet Models

- Internal Shocks (Marscher & Gear 1985, Spada et al. 2001, Sokolov et al. 2004, Dermer & Böttcher 2010, Joshi & Böttcher 2011, Chen et al. 2011, 2012)

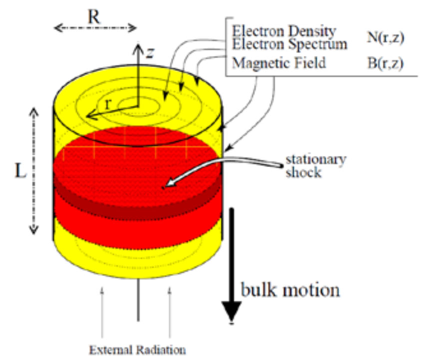

- Radially stratified jets (spine-sheath model, Ghisellini et al. 2005, Ghisellini & Tavecchio 2008)

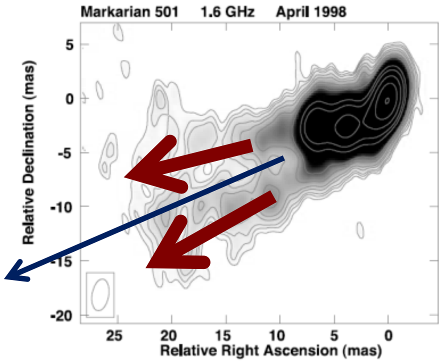

- Decelerating Jet Model (Georganopoulos & Kazanas 2003)

- Mini-jets-in-jet (magnetic reconnection – Giannios et al.)

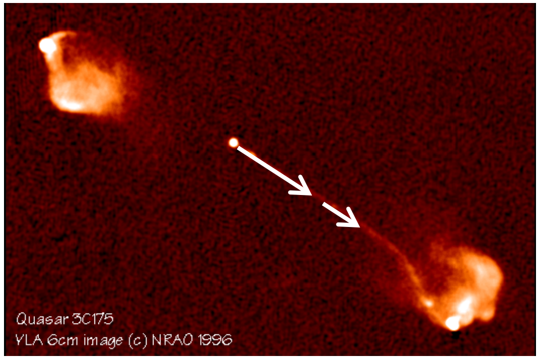

- Extended-jet models (e.g., Potter & Cotter 2012, 2013; Richter & Spanier 2015)

Polarization Angle Swings

- Optical + γ-ray variability of LSP blazars often correlated
- Sometimes O/γ flares correlated with increase in optical polarization and multiple rotations of the polarization angle (PA)

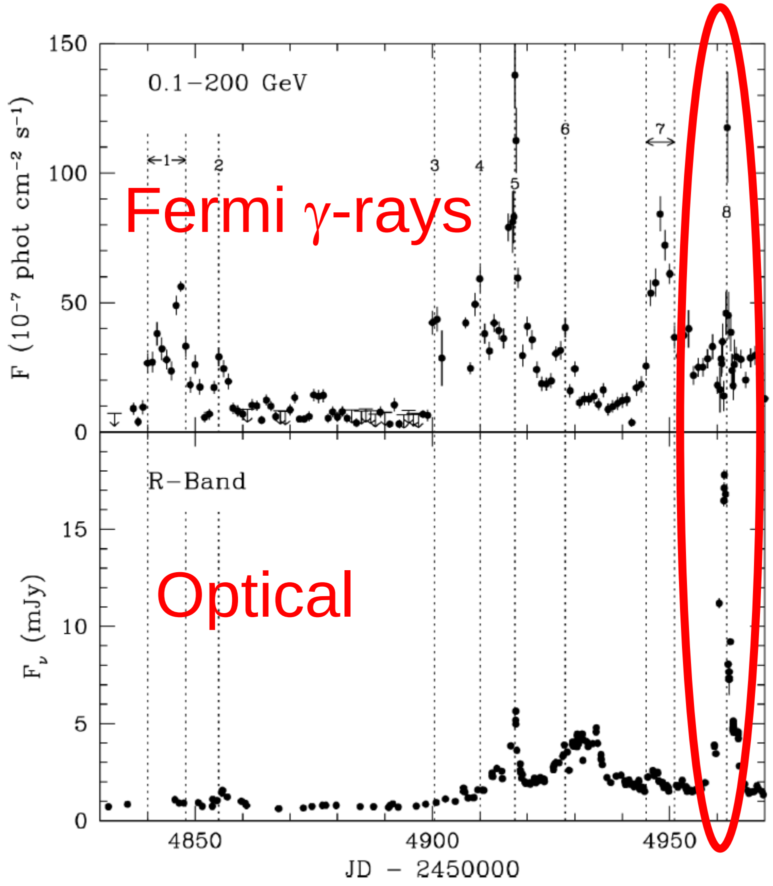

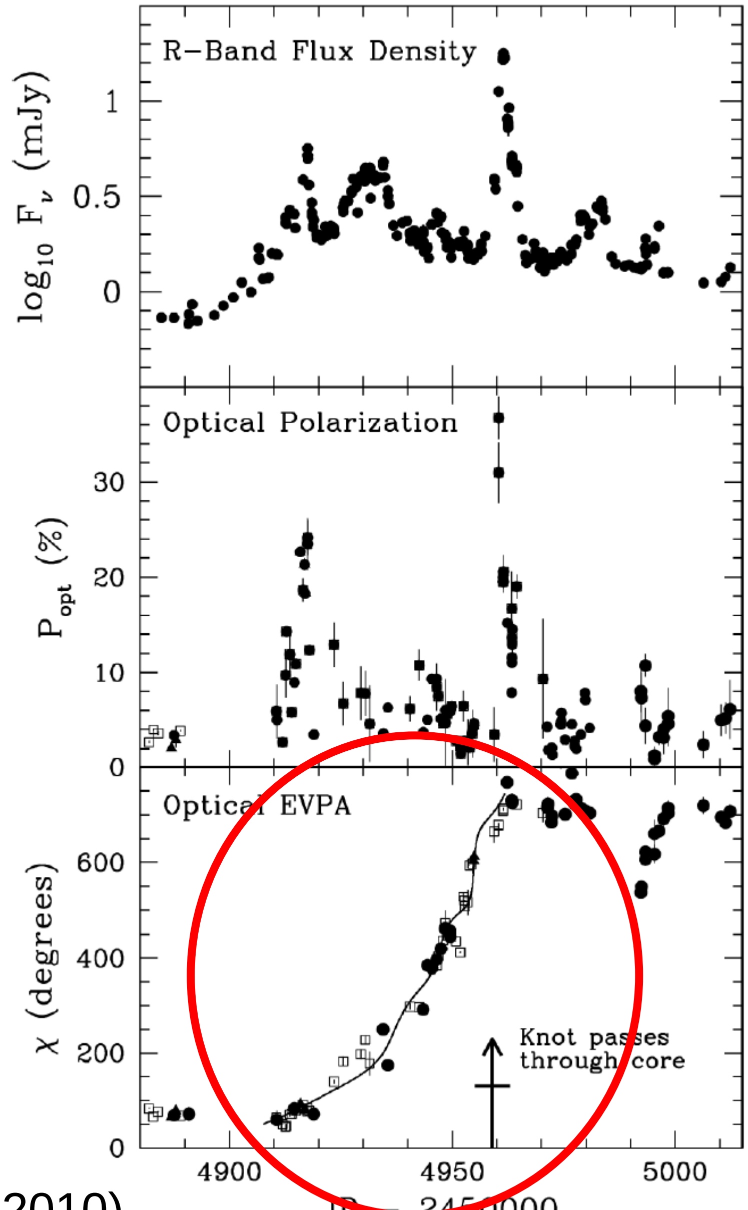

PKS 1510-089 (Marscher et al. 2010)

Previously Proposed Interpretations:

- Helical magnetic fields in a bent jet
- Helical streamlines, guided by a helical magnetic field
- Turbulent Extreme Multi-Zone Model (Marscher 2014)

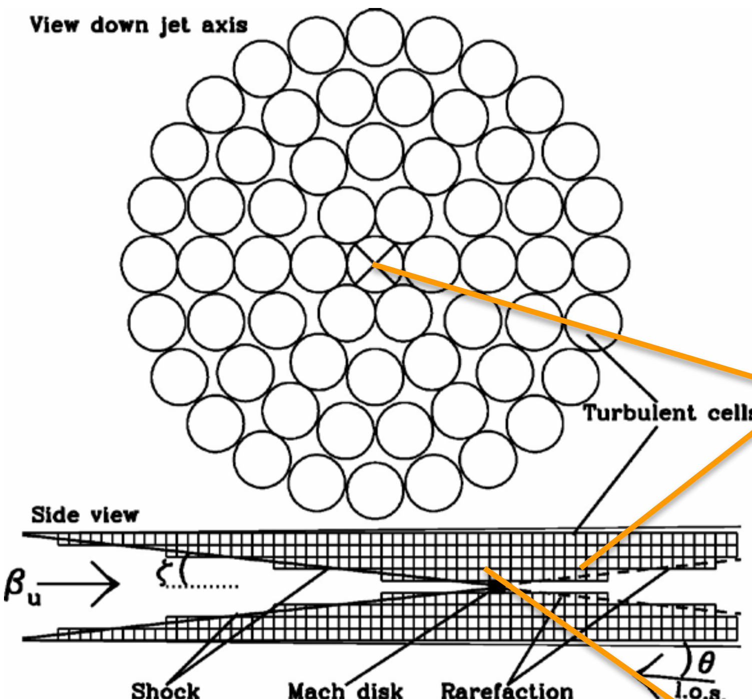

Mach disk

Looking at the jet from the side

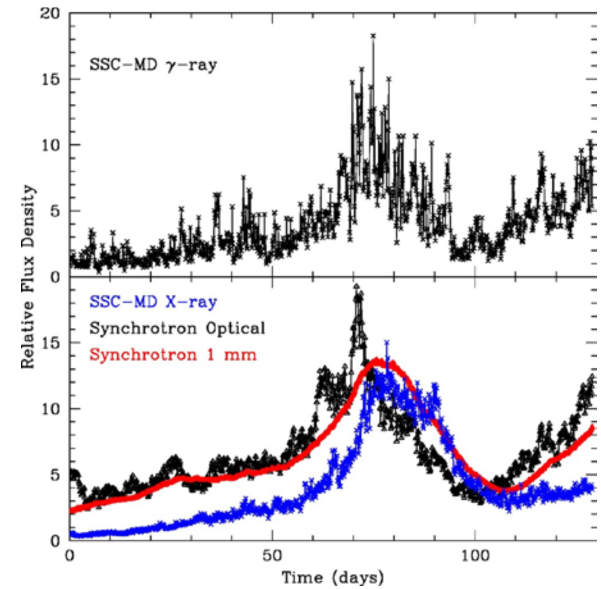

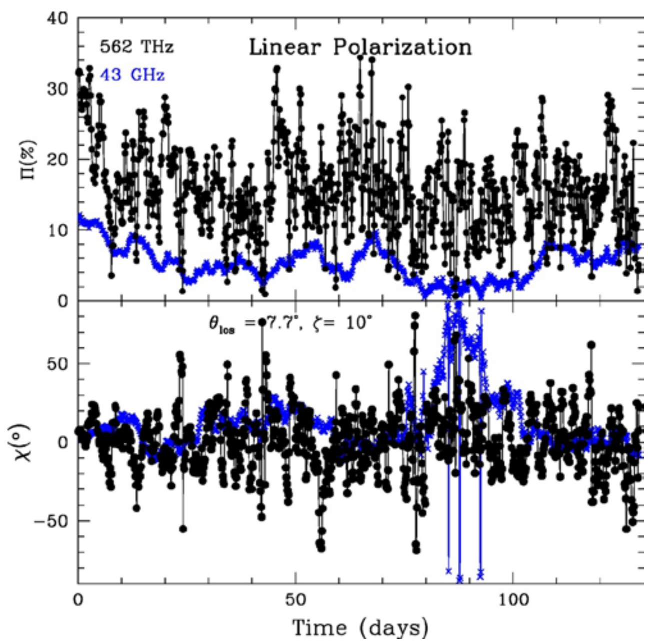

Tracing Synchrotron Polarization in the Internal Shock Model

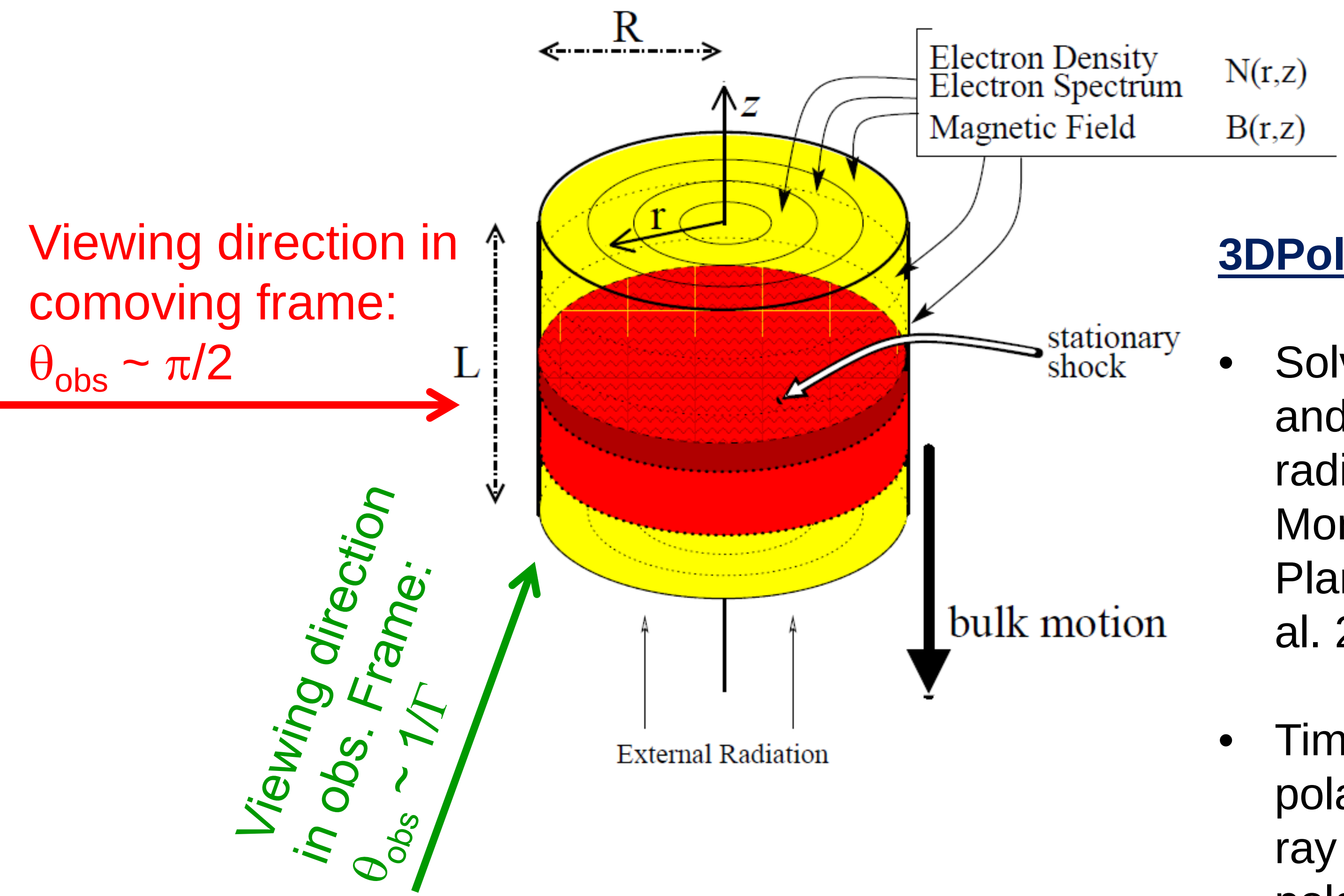

3DPol (Zhang et al. 2014)

- Solve electron dynamics and (unpolarized) radiation transfer with Monte-Carlo / Fokker-Planck scheme (Chen et al. 2011, 2012)
- Time-dependent, polarization-dependent ray tracing for polarization signatures

Light Travel Time Effects

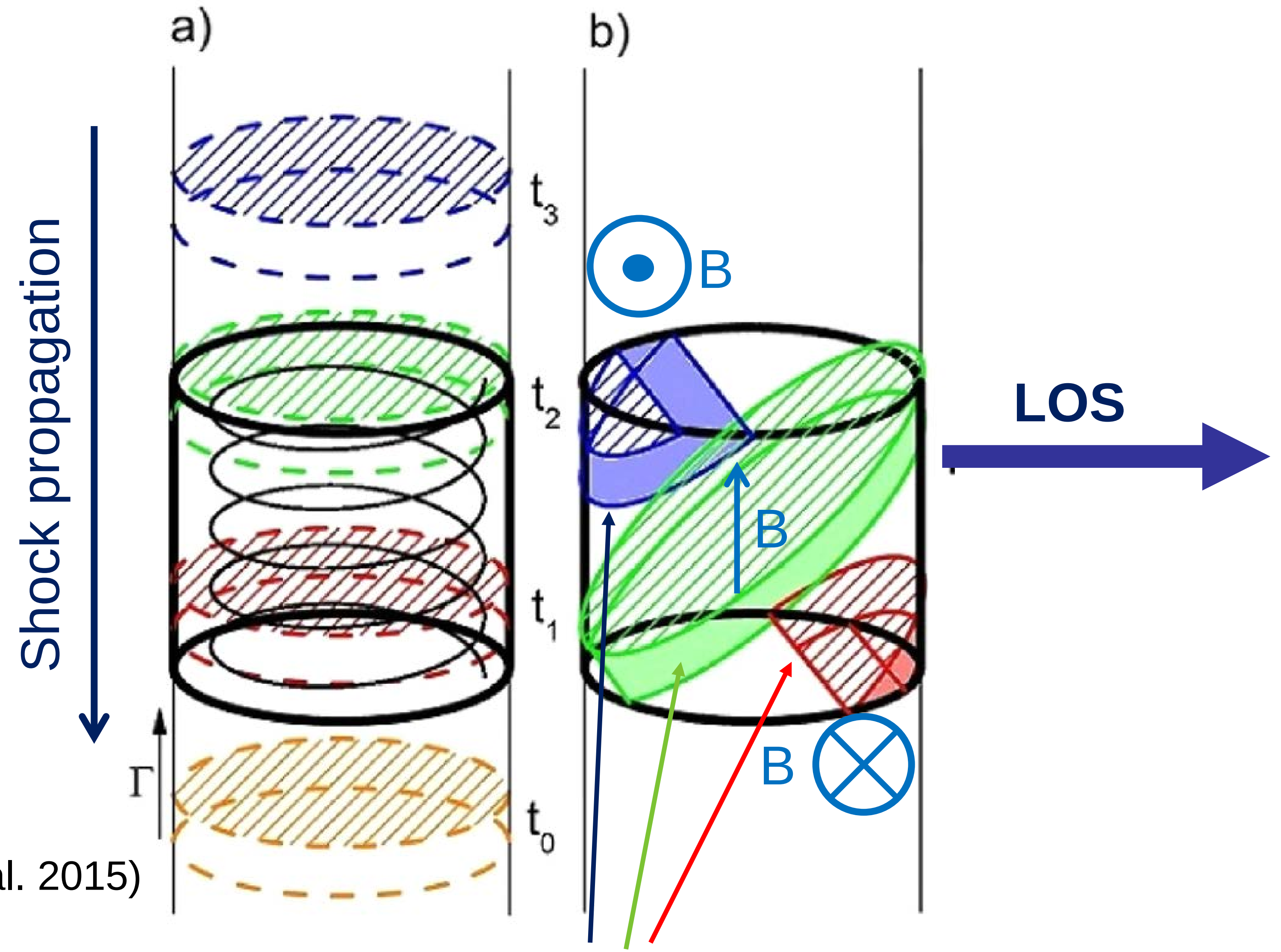

(Zhang et al. 2015)

Shock positions at equal photon-arrival times at the observer

Application to the FSRQ 3C279

Simultaneous optical + γ-ray flare, correlated with a 180º polarization-angle rotation .

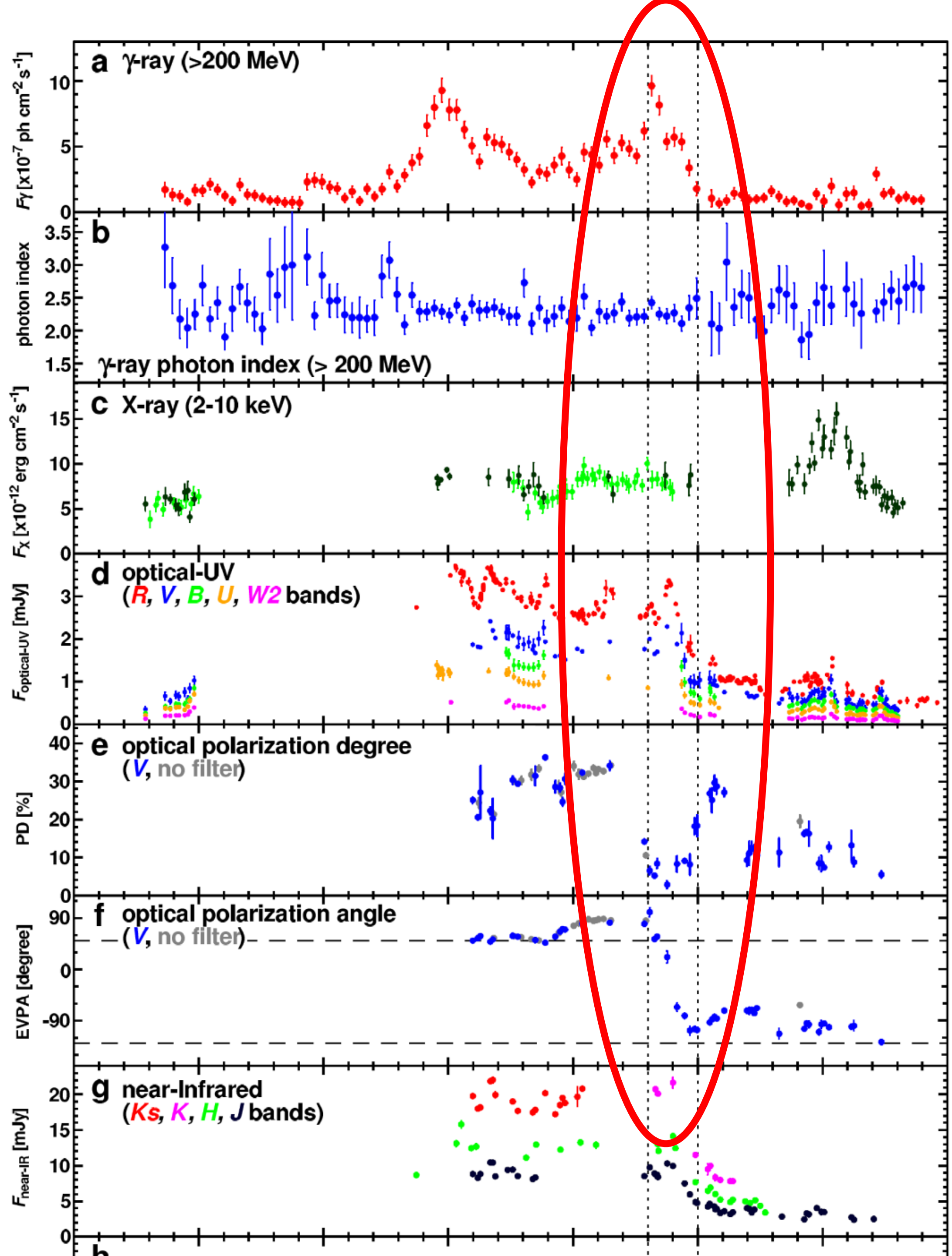

(Abdo et al. 2009)

Application to 3C279

Simultaneous fit to SEDs, light curves, polarization-degree and polarization-angle swing

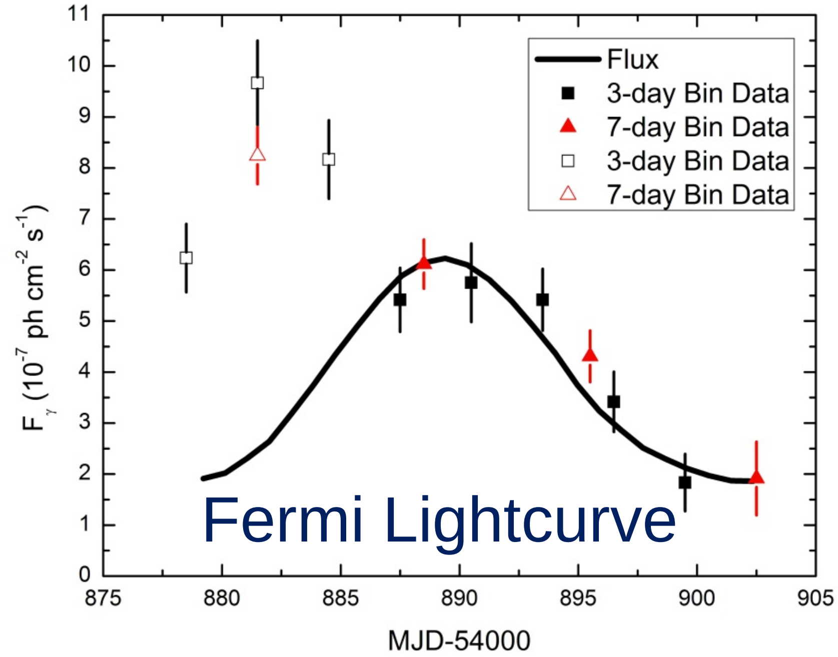

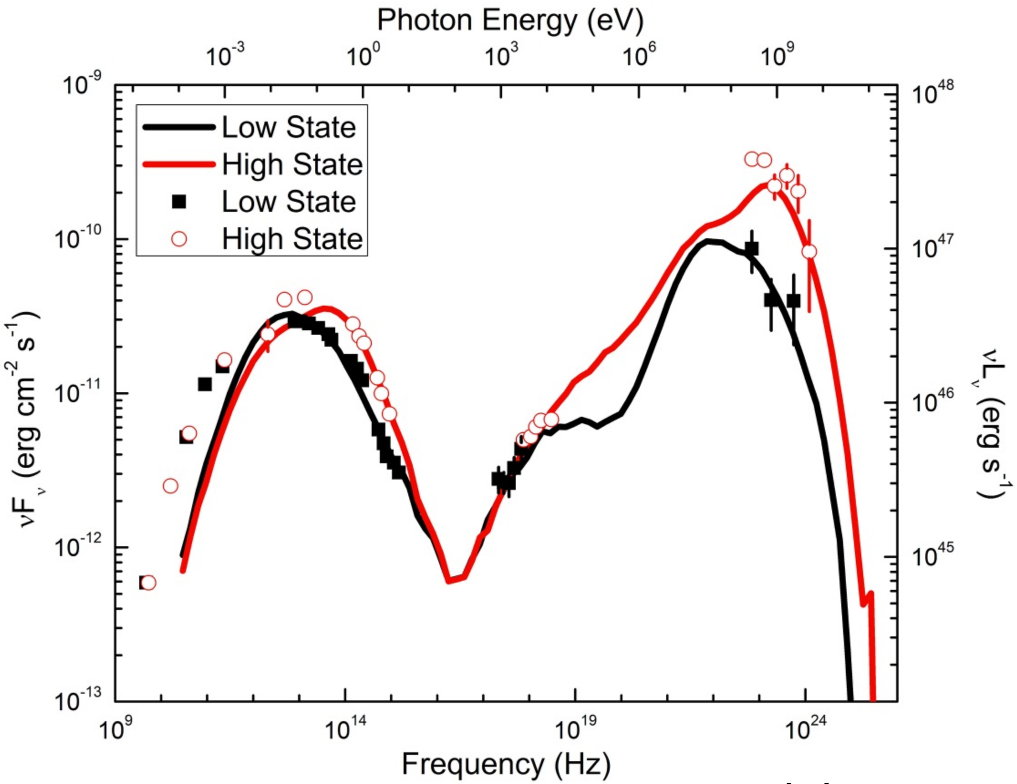

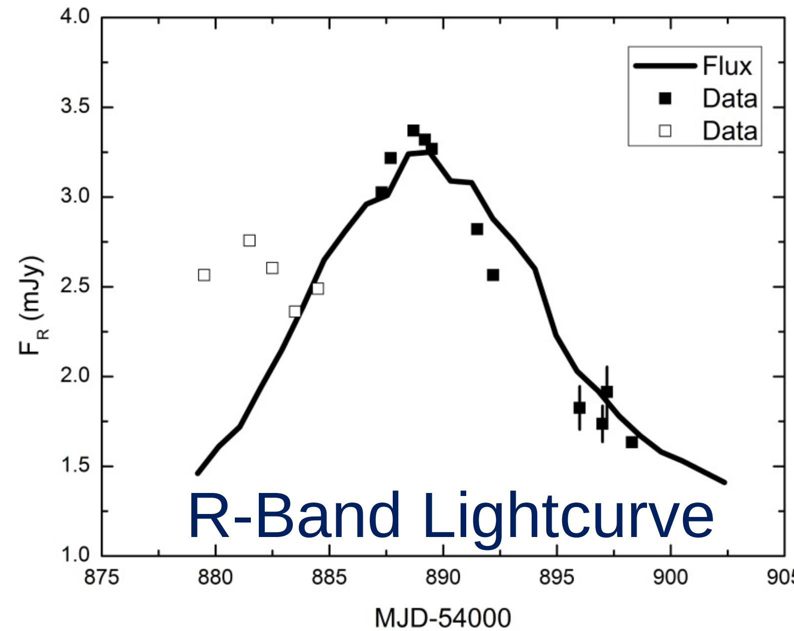

(Zhang et al. 2015)

Application to 3C279

Requires particle acceleration
and reduction of magnetic field,
as expected in magnetic reconnection!

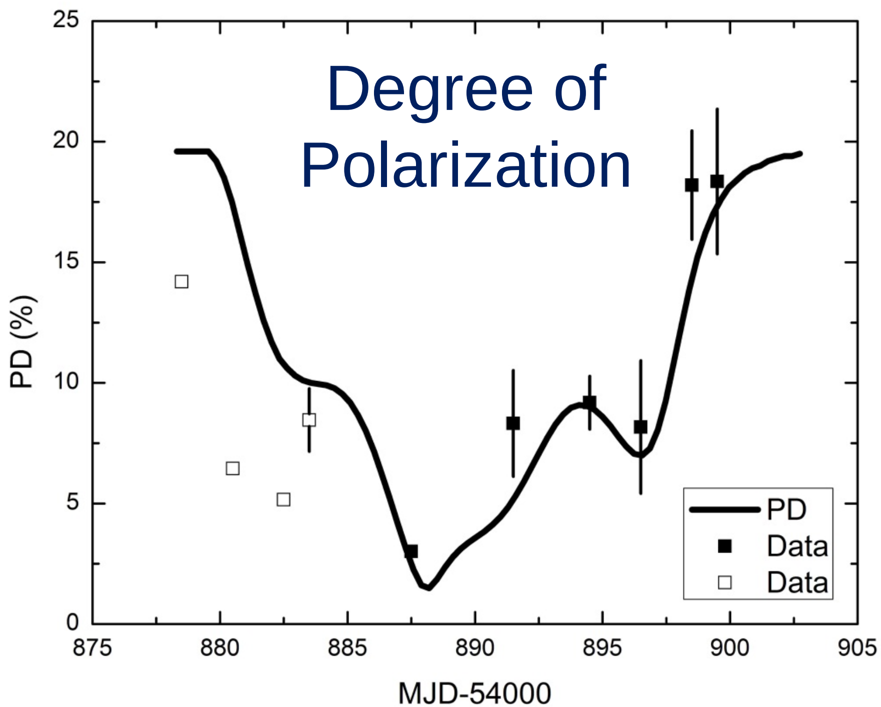

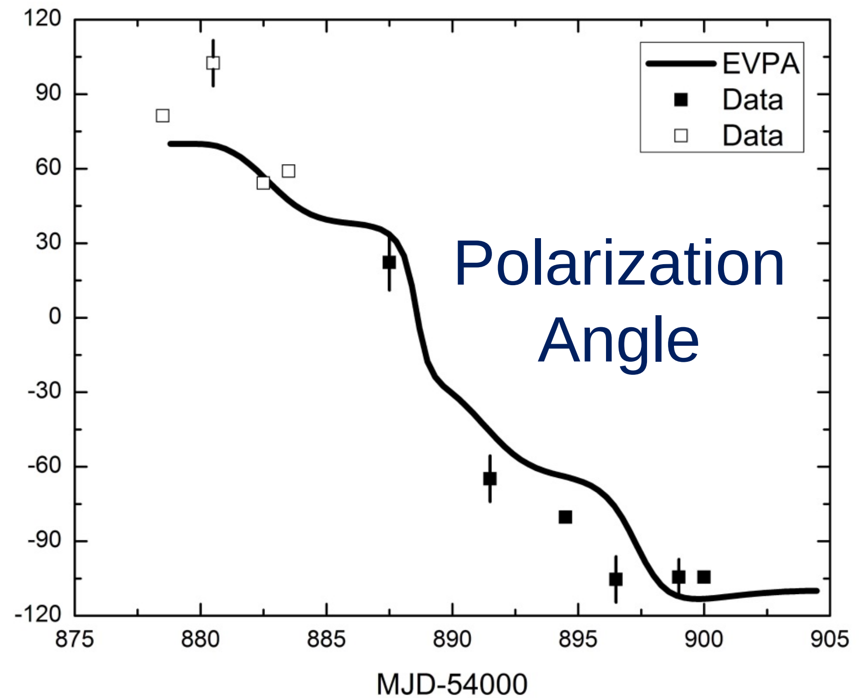

(Zhang et al. 2015)

Coupling to Realistic MHD Simulations

- Ideal RMHD Simualtions (LA-COMPASS [LANL]) of relativistic shocks
- Jets initially pervaded by purely helical B-fields with magnetization parameter

$$\sigma = \frac{E_{em}}{h} \qquad E_{em} = \frac{E^2+B^2}{8\pi} \qquad h = \rho c^2 + \frac{\gamma p}{\gamma - 1}$$

- Fixed fraction of liberated energy converted to the injection of power-law non-thermal electrons
- Follow particle evolution, radiation, and time-dependent polarization signatures using 3DPol.

(Zhang et al. 2016)

Simulation Setup

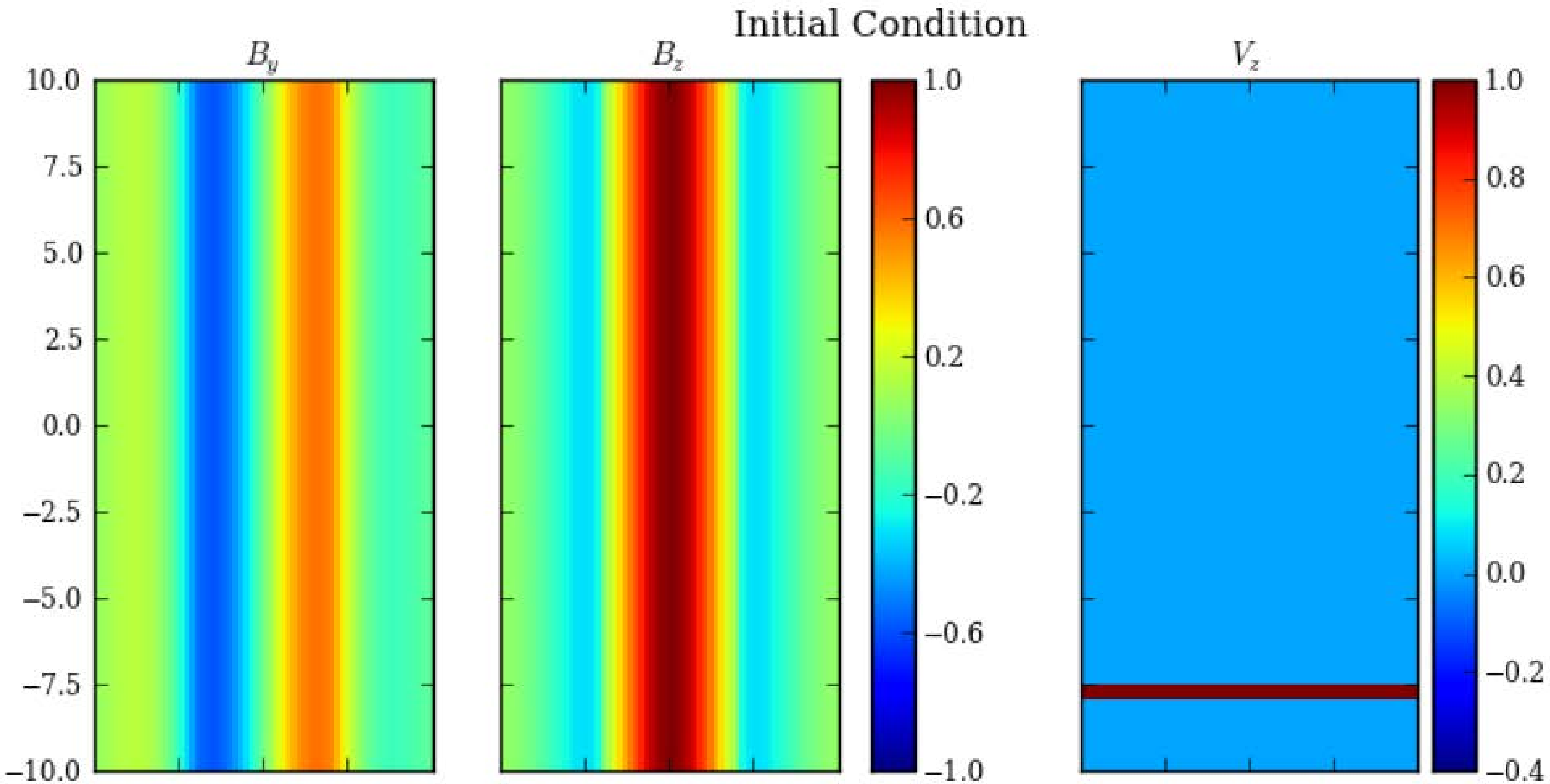

(Zhang et al. 2016)

B-Field Evolution

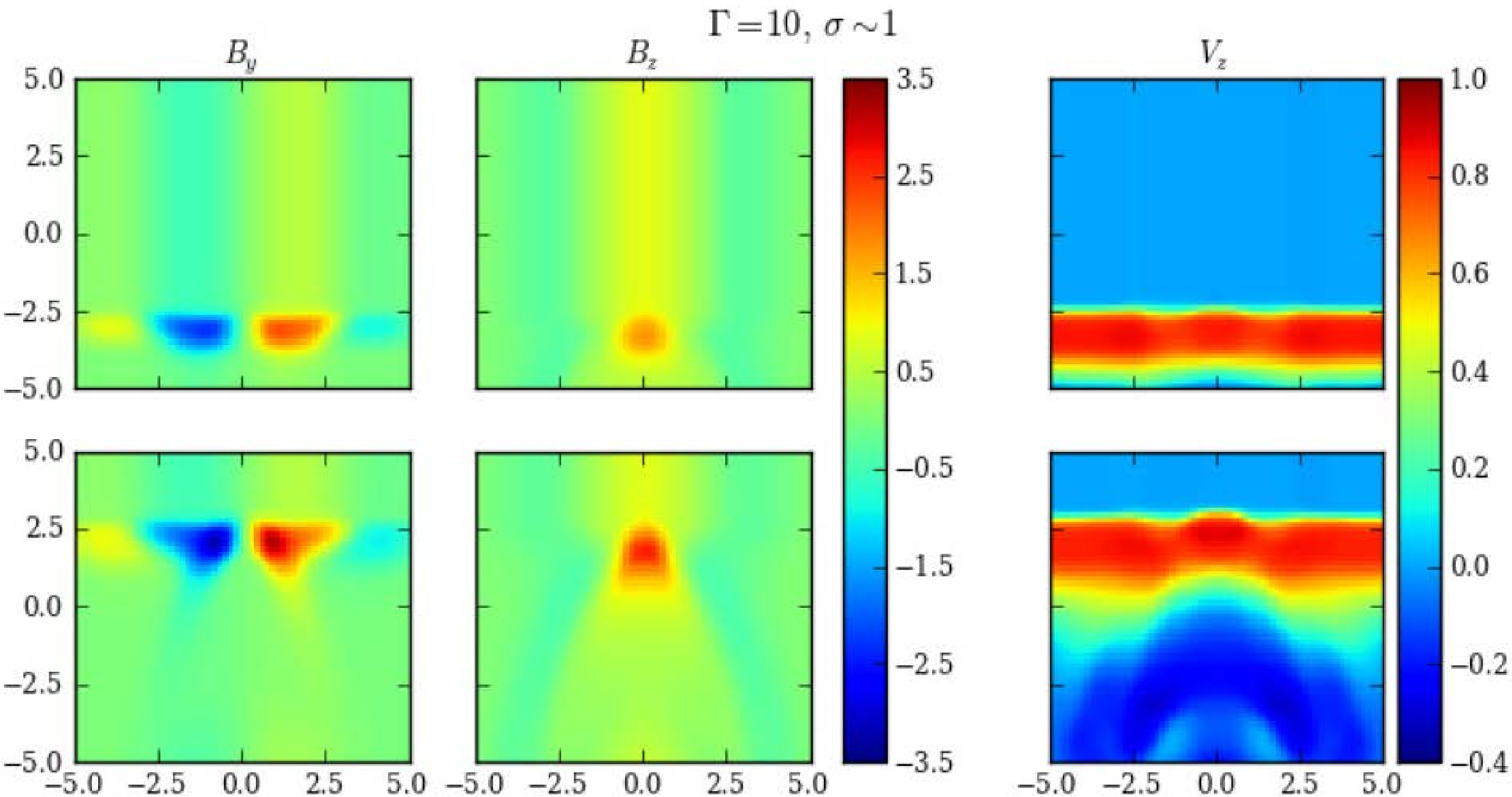

(Zhang et al. 2016)

High / moderate magnetization

- Weak shock
- velocity field strongly disturbed
- B-field restored to its original topology after passage of the shock

B-Field Evolution

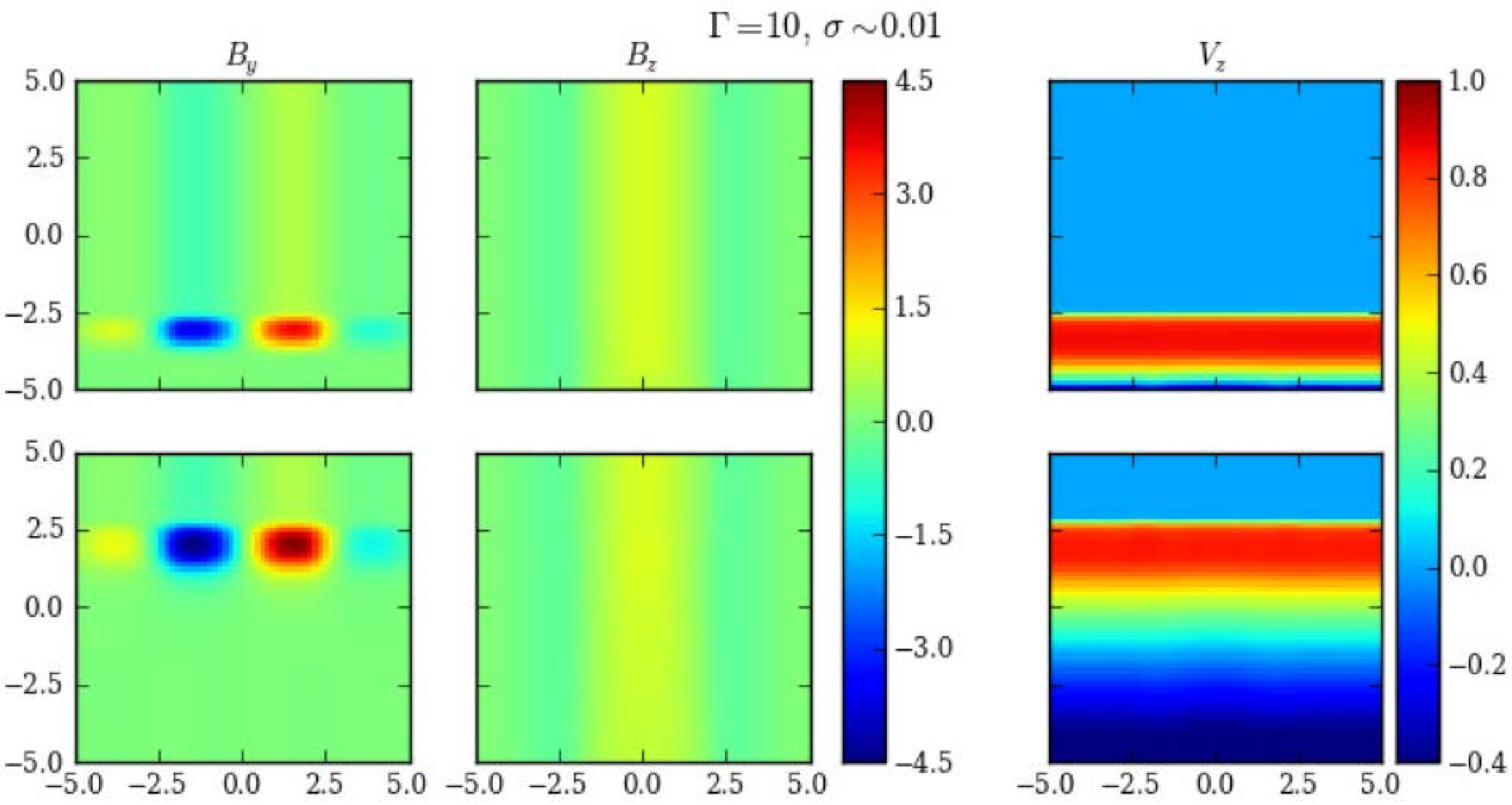

(Zhang et al. 2016)

Low magnetization

- Strong shock
- velocity field almost undisturbed
- B-field topology significantly altered after passage of the shock

Polarization Signatures

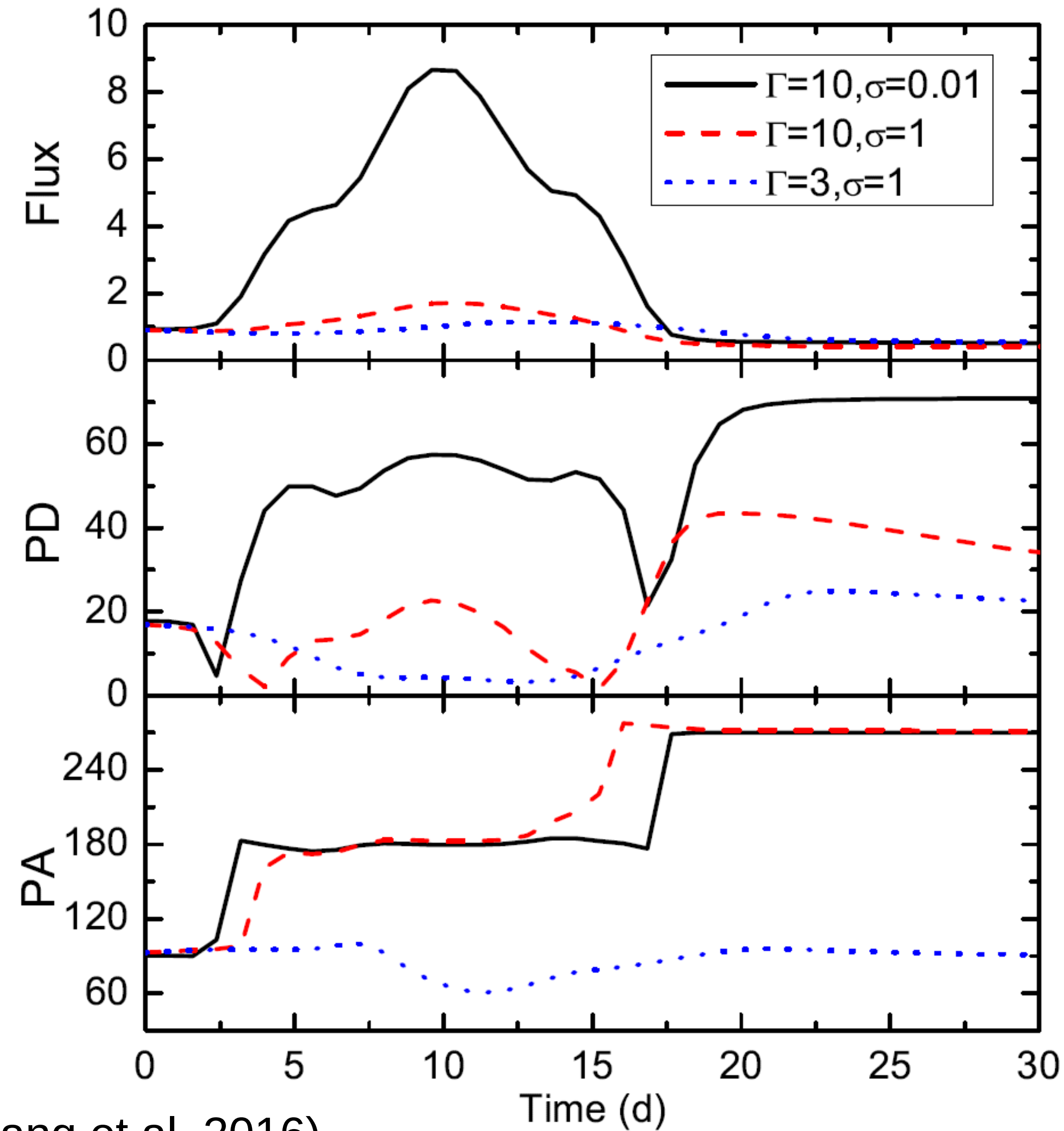

(Zhang et al. 2016)

- PA swings with PD recovering to its pre-flare level require high / moderate magnetization ($\sigma \geq 1$) - otherwise B-field is not restored to its original topology
- Significant flares require strong shocks, i.e., moderate / high shock speed and moderate / low magnetization

Summary

1. Both leptonic and hadronic models can generally fit blazar SEDs well. Possible distinguishing diagnostics: Variability, polarization, neutrinos

2. Simultaneous SED + MW-light-curve fitting of 3C454.3 (Nov. 2010) favours a lepto-hadronic model (but requires large jet power, $L_p \sim L_{Edd}$)

3. Significant high-energy polarization is a signature of hadronic models.

4. Polarization-angle swings correlated with MW flares are possible in a straight jet, pervaded by a helical magnetic field, in an internal shock model. This requires fast (strong) shocks in a moderately magnetized ($\sigma \sim 1$) plasma.

Happy Star Wars Day!

Blazars

- Class of AGN consisting of BL Lac objects and gamma-ray bright quasars
- Rapidly (often intra-day) variable

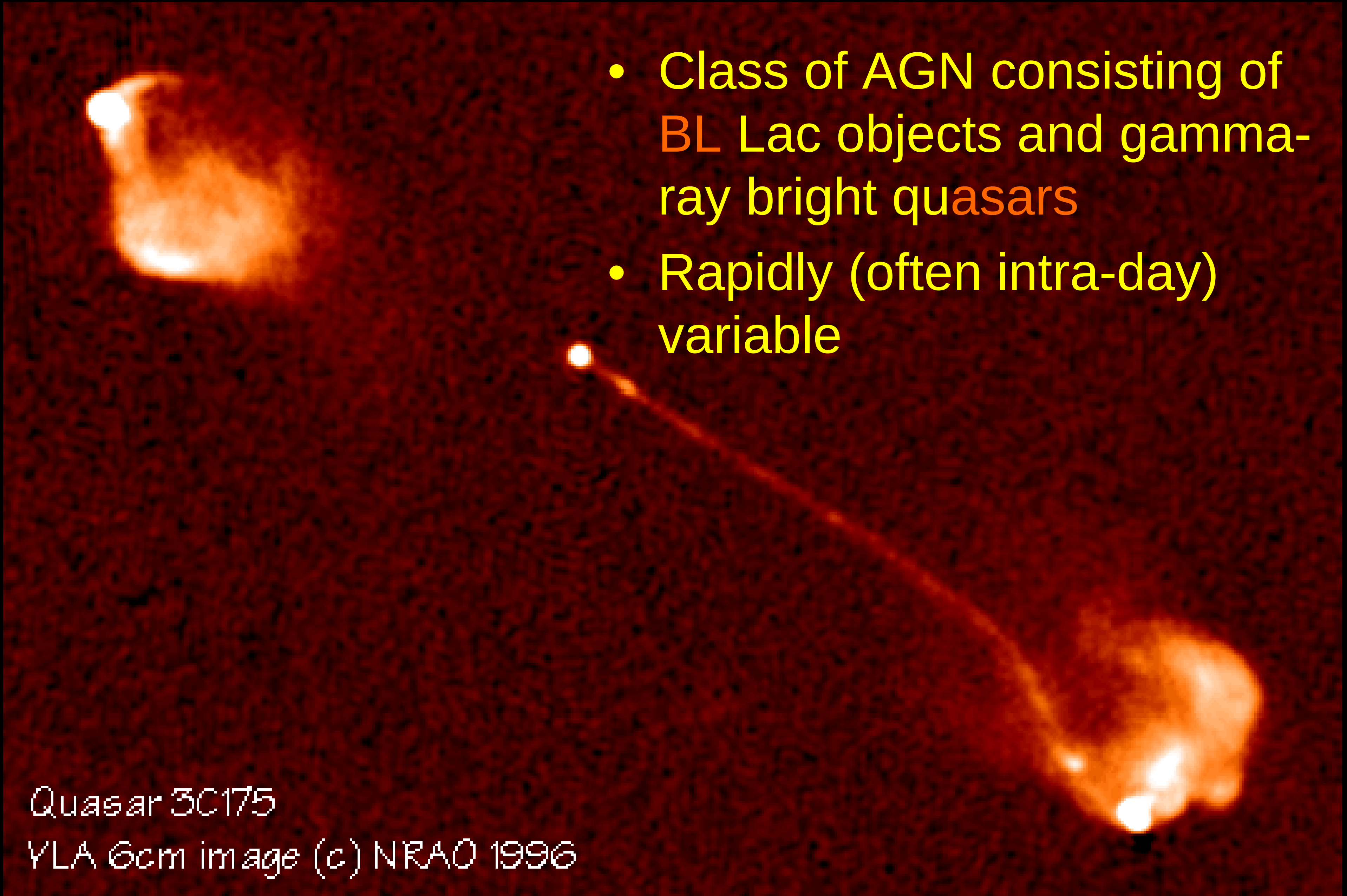

Blazar Variability: Example: The Quasar 3C279

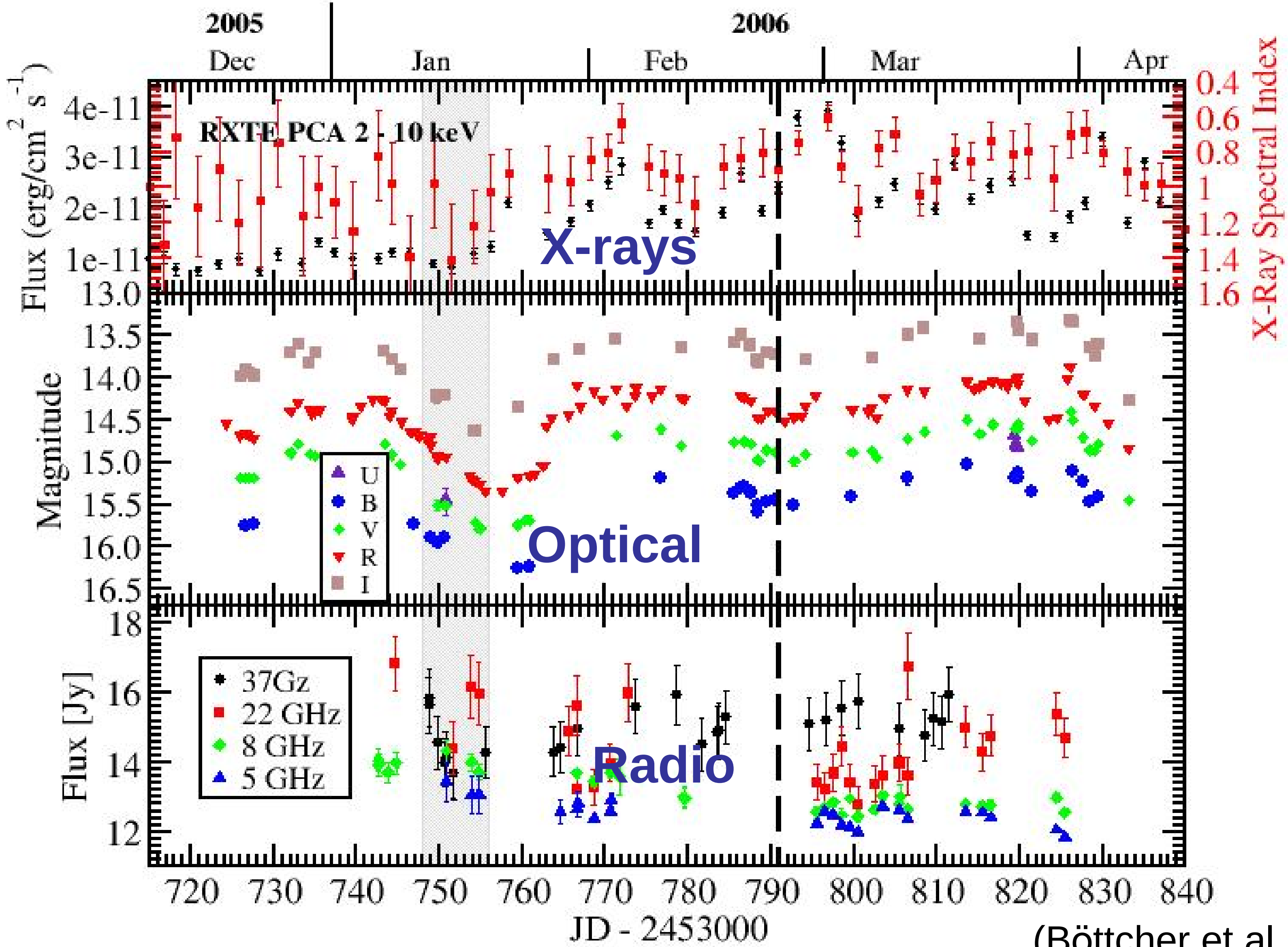

(Böttcher et al. 2007)

Blazar Variability:
Variability of PKS 2155-304

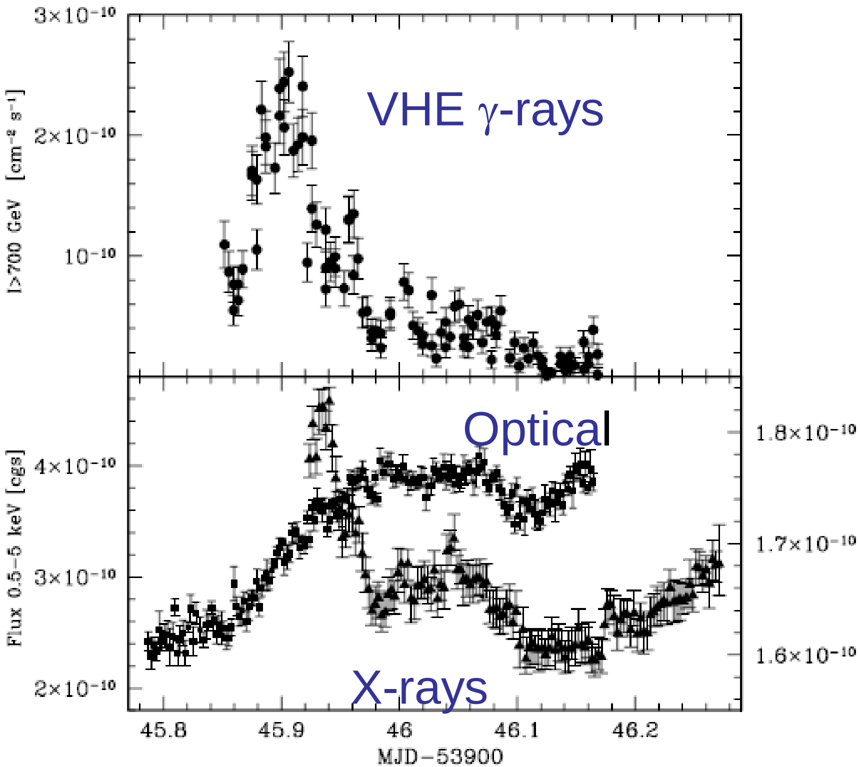

(Costamante et al. 2008)

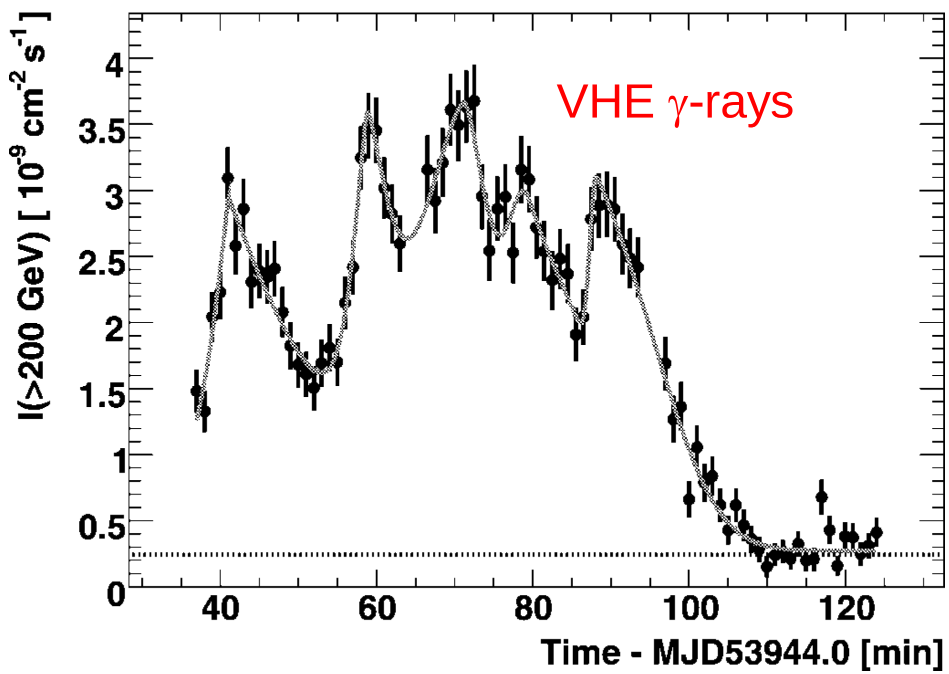

(Aharonian et al. 2007)

VHE γ-ray variability on time scales as short as a few minutes!

VHE γ-ray and X-ray variability often closely correlated

Blazars

- Class of AGN consisting of BL Lac objects and gamma-ray bright quasars
- Rapidly (often intra-day) variable
- Strong gamma-ray sources

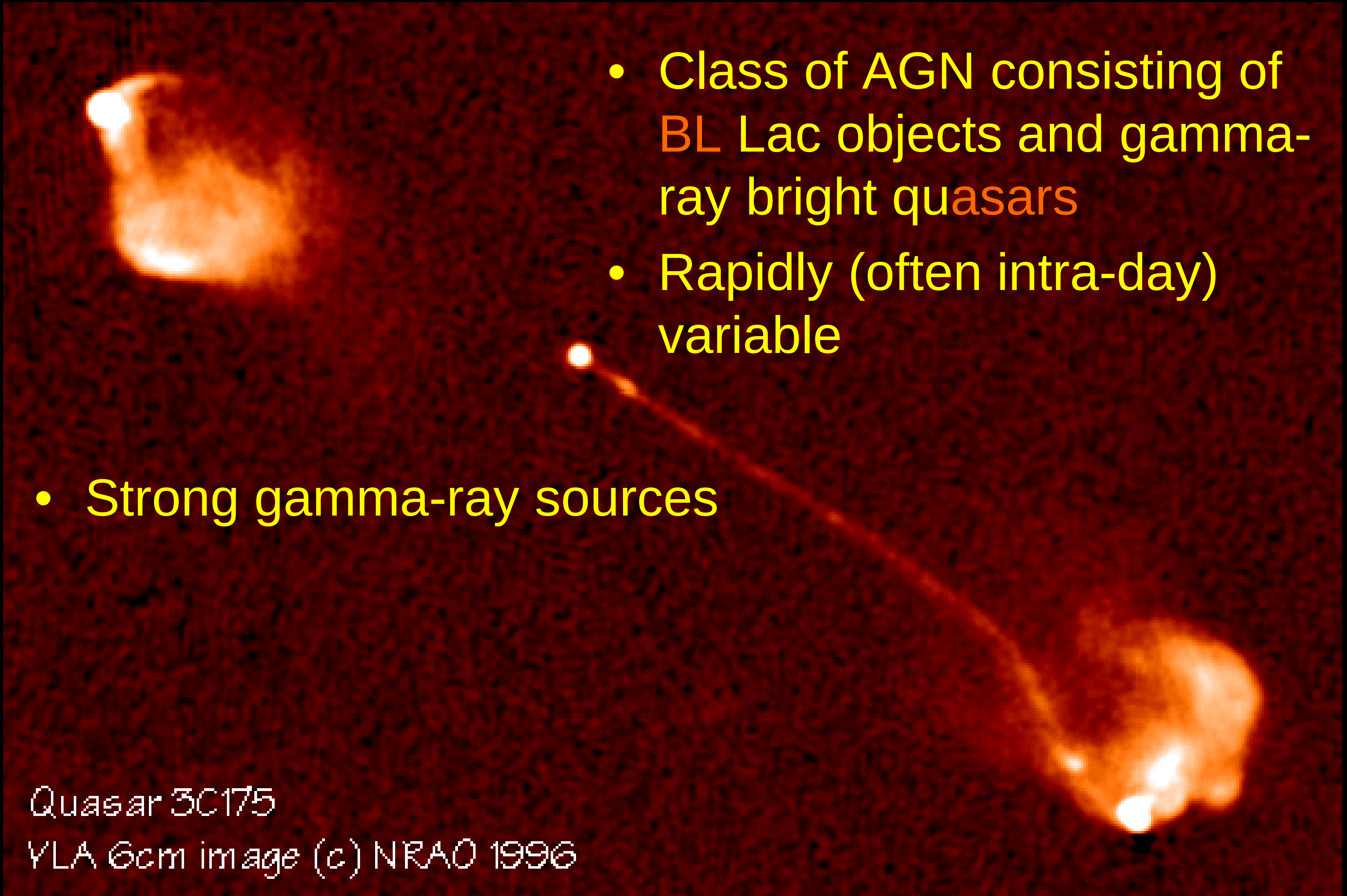

Blazar Spectral Energy Distributions (SEDs)

3C66A

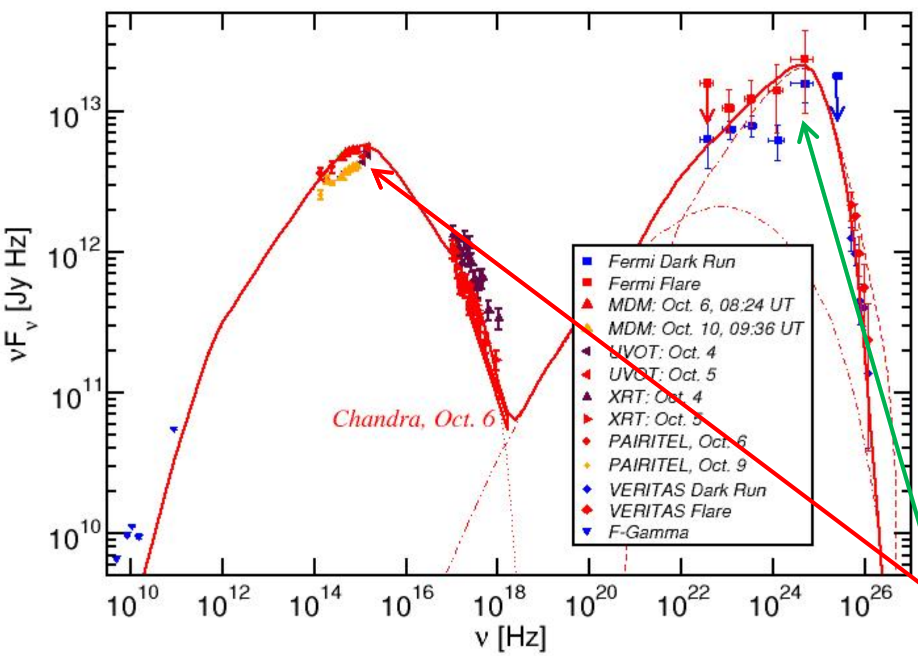

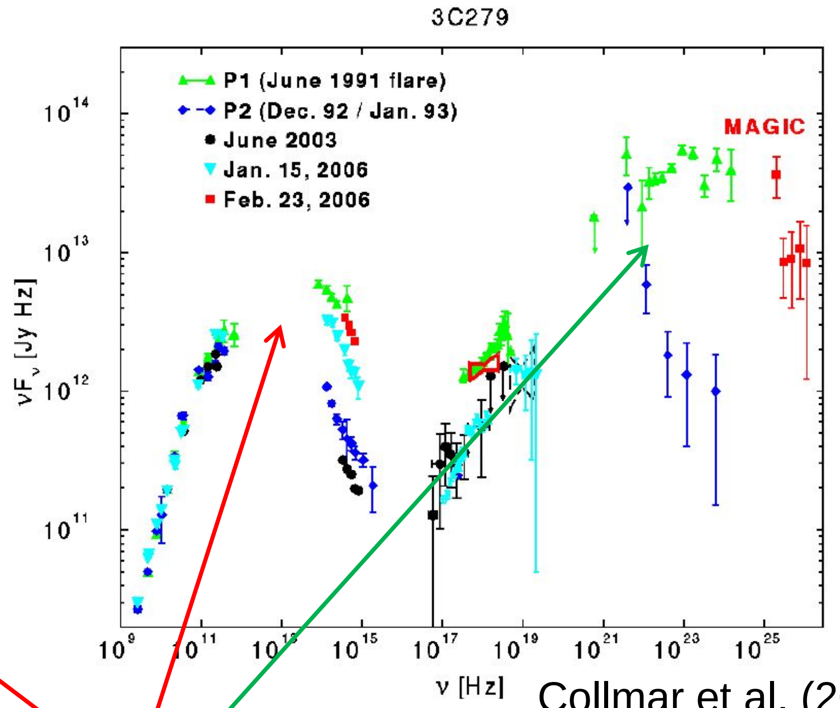

Collmar et al. (2010)

Non-thermal spectra with two broad bumps:

- Low-energy (probably synchrotron): radio-IR-optical(-UV-X-rays)
- High-energy (X-ray – γ-rays)

Superluminal Motion

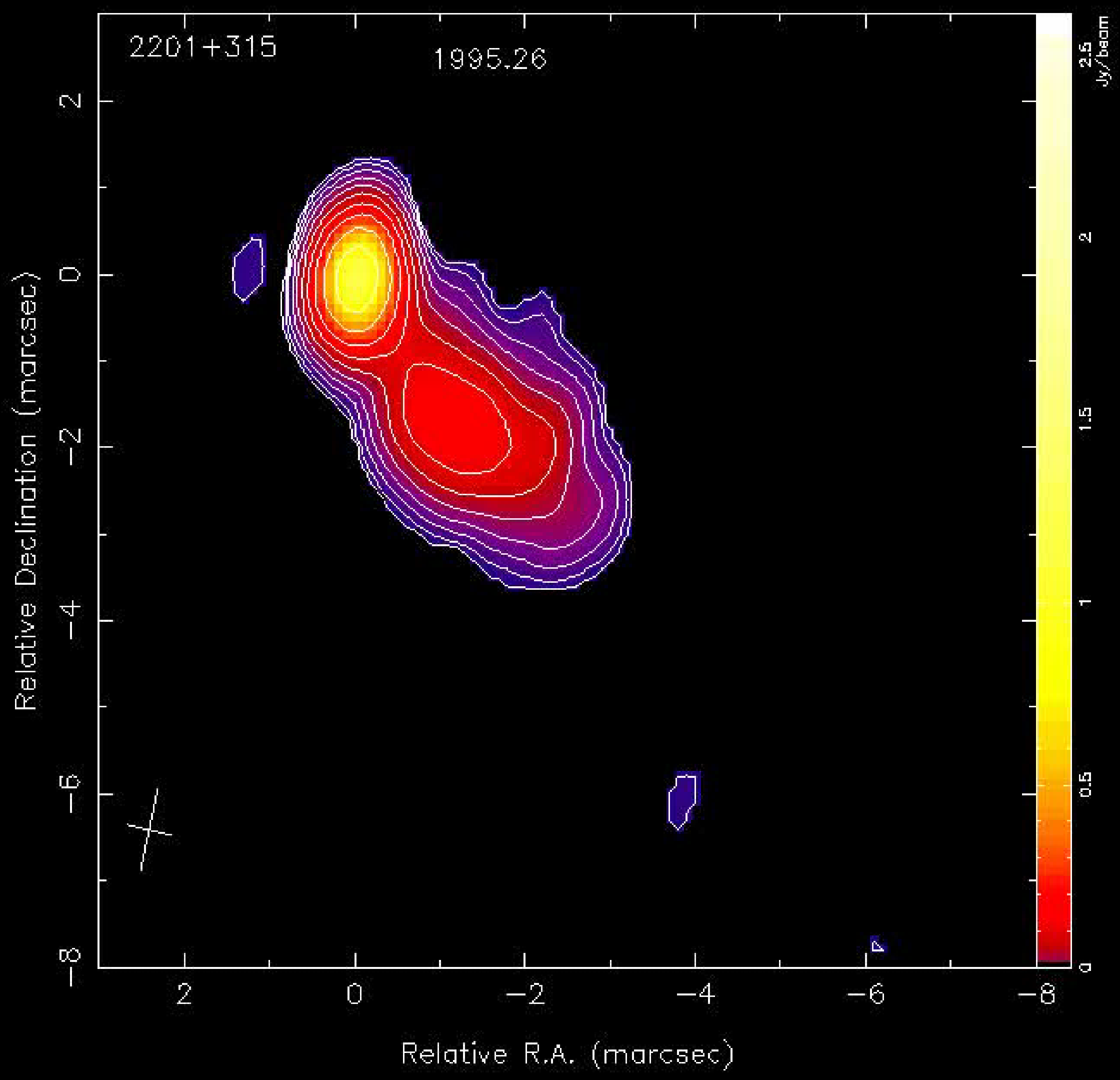

(The MOJAVE Collaboration)

Superluminal Motion

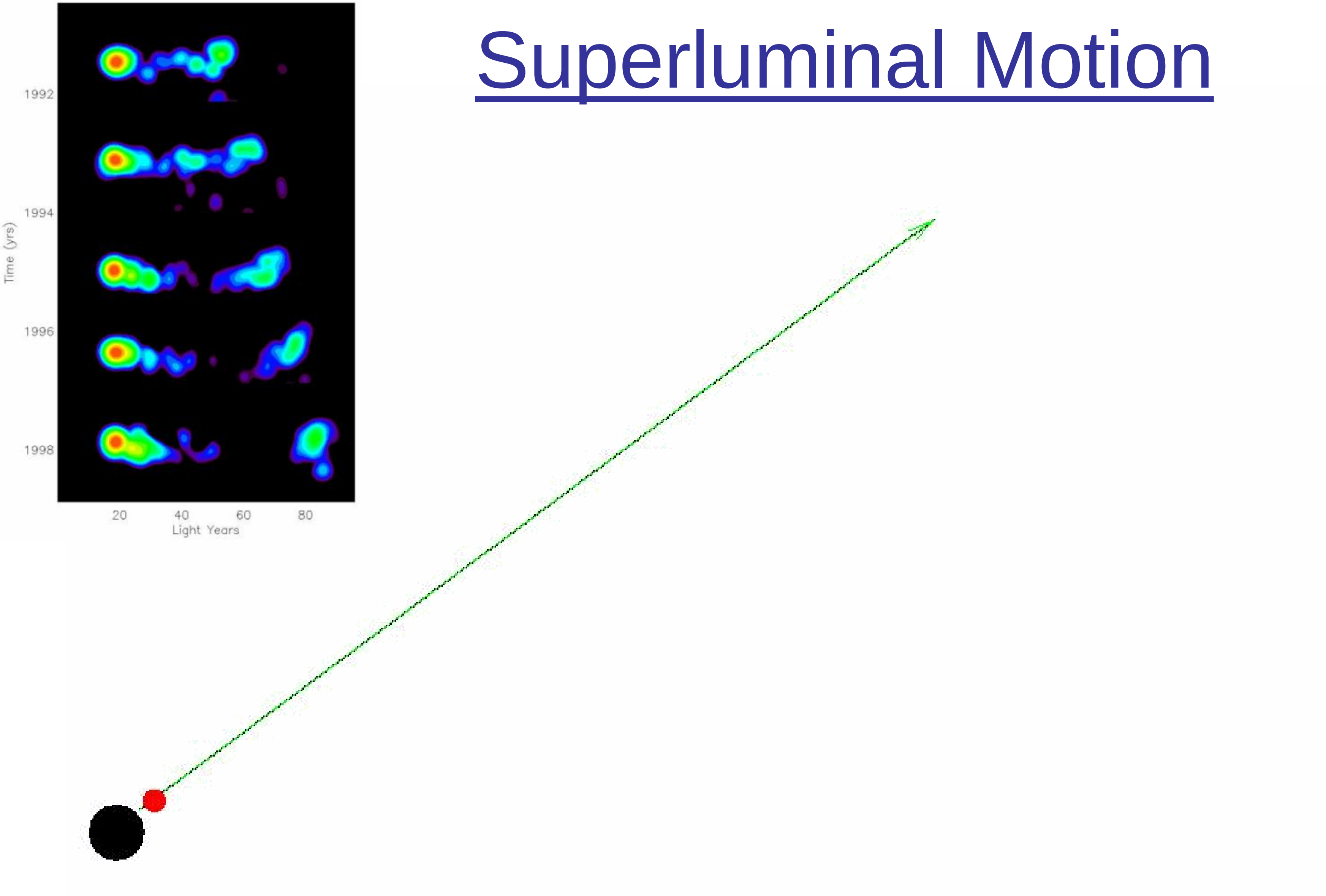

Apparent motion at up to ~ 40 times the speed of light!

Spectral modeling results along the Blazar Sequence: Leptonic Models

High-frequency peaked BL Lac (HBL):

Low magnetic fields (~ 0.1 G);

High electron energies (up to TeV);

Large bulk Lorentz factors ($\Gamma > 10$)

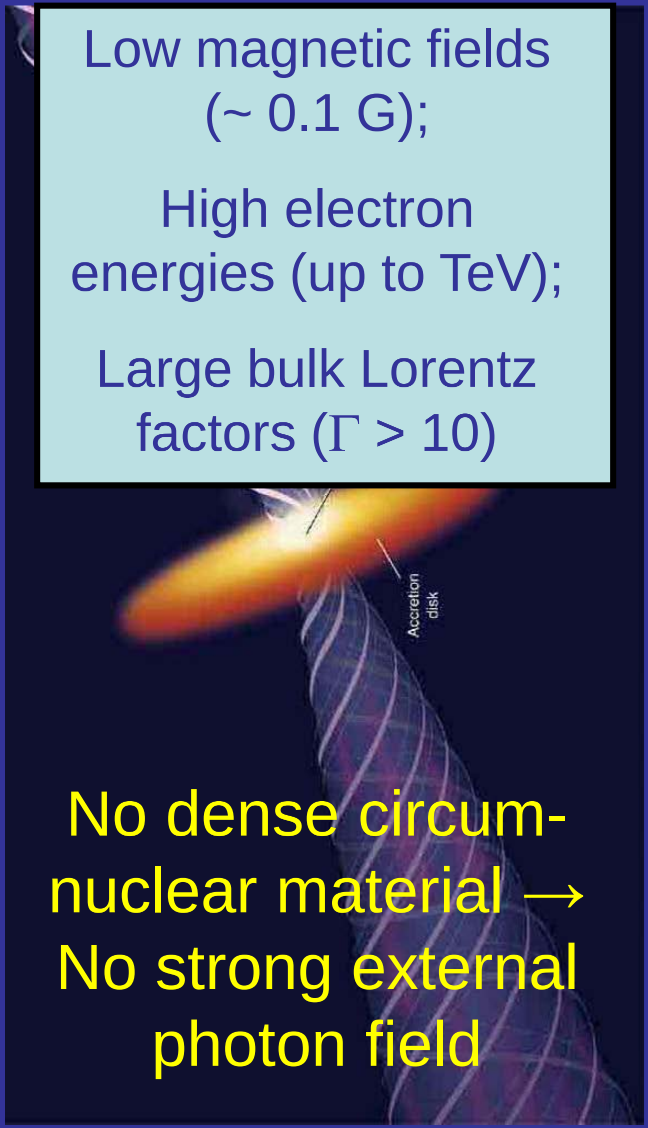

No dense circum-nuclear material → No strong external photon field

The "classical" picture

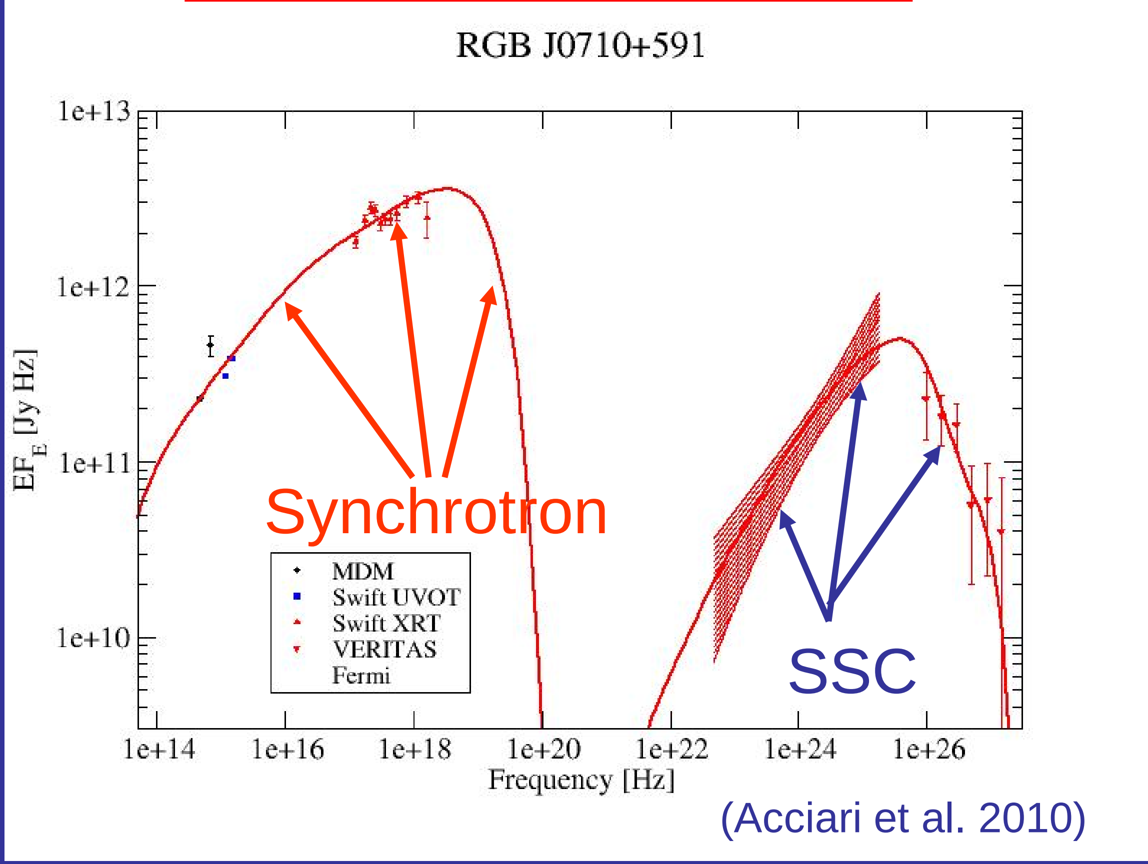

(Acciari et al. 2010)

Spectral modeling results along the Blazar Sequence: Leptonic Models

High magnetic fields (~ a few G);

Lower electron energies (up to GeV);

Lower bulk Lorentz factors ($\Gamma \sim 10$)

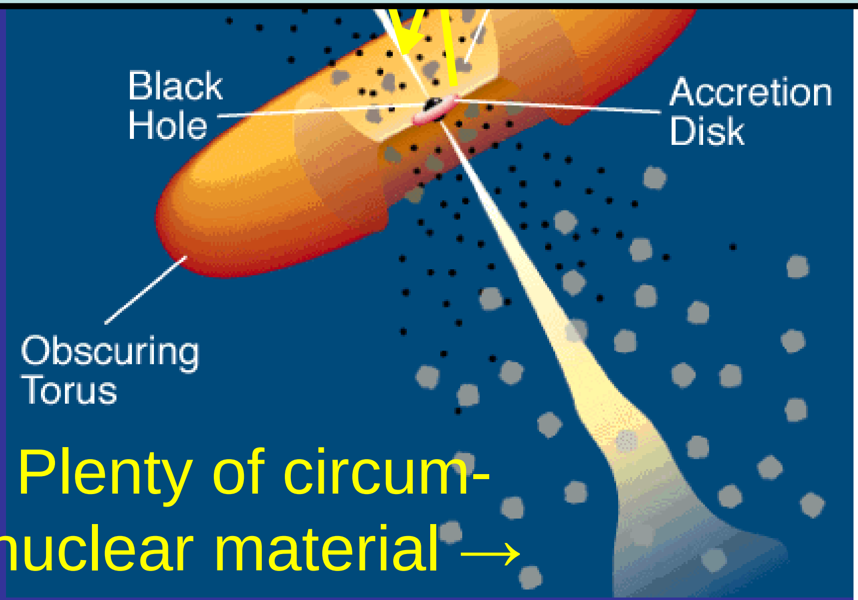

Plenty of circum-nuclear material $\rightarrow$ Strong external photon field

FSRQ

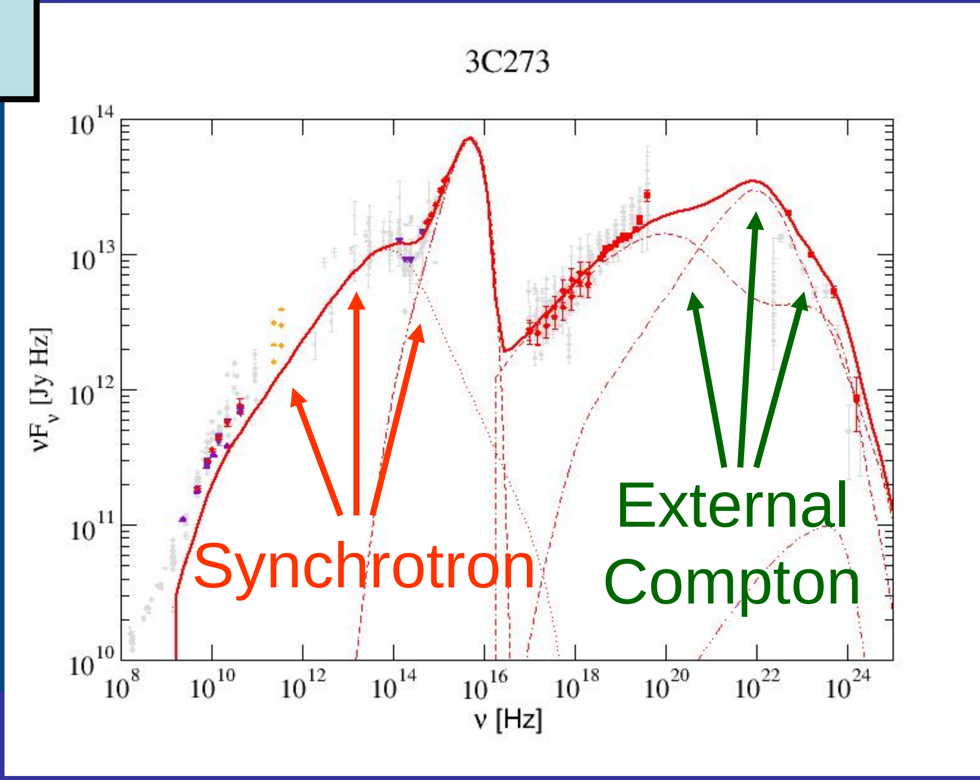

Constraints from Observations

If energy-dependent (spectral) time lags are related to energy-dependent synchrotron cooling time scale:

$d\gamma/dt = -\nu_0\gamma^2$ with $\nu_0 = (4/3)\, c\, \sigma_T\, u'_B\, (1 + k)$

and $k = u'_{ph}/u'_B$ (Compton Dominance Parameter)

$t_{cool} = \gamma/|d\gamma/dt| = 1/(\nu_0\gamma)$

$\nu_{sy} = 3.4 \cdot 10^6\, (B/G)\, (\delta/(1+z))\, \gamma^2$ Hz

=> $\Delta t_{cool} \sim B^{-3/2}\, (\delta/(1+z))^{1/2}\, (1 + k)^{-1} (\nu_1^{-1/2} - \nu_2^{-1/2})$

=> Measure time lags between frequencies ν_1, ν_2
→ estimate Magnetic field (modulo $\delta/[1+z]$)!

(Takahashi et al. 1996)

Distinguishing Diagnostic: Variability

- Time-dependent leptonic one-zone models produce correlated synchrotron + gamma-ray variability (Mastichiadis & Kirk 1997, Li & Kusunose 2000, Böttcher & Chiang 2002, Moderski et al. 2003, Diltz & Böttcher 2014)

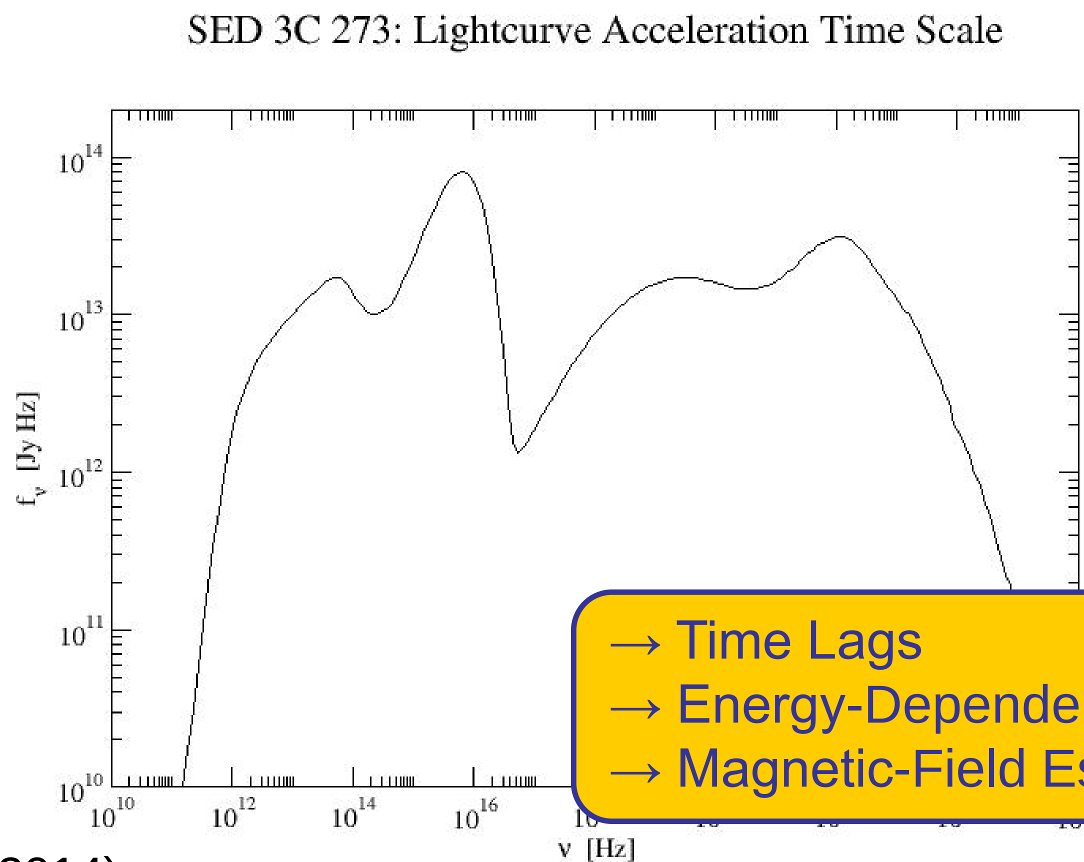

→ Time Lags
→ Energy-Dependent Cooling Times
→ Magnetic-Field Estimate!

Diltz & Böttcher (2014)

Correlated Multiwavelength Variability in Leptonic One-Zone Models

Example: Variability from short-term increase in 2nd-order-Fermi acceleration efficiency

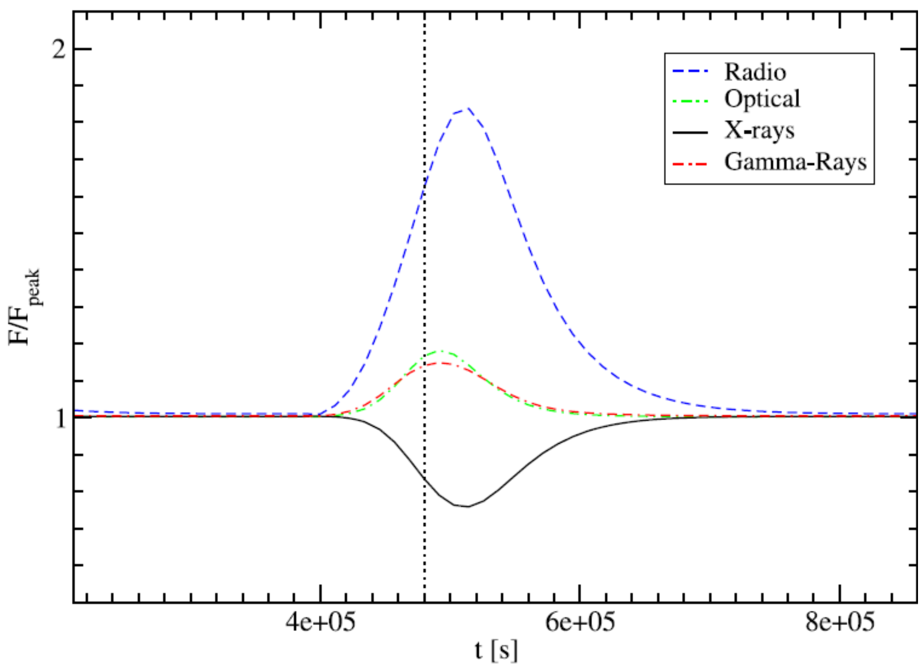

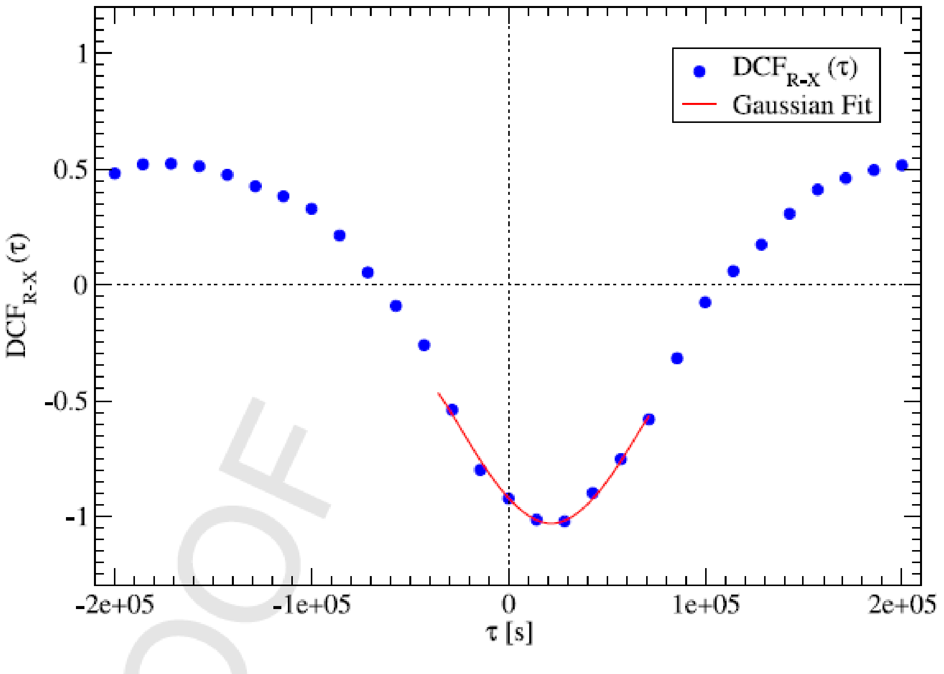

X-rays anti-correlated with radio, optical, γ-rays; delayed by ~ few hours.

(Diltz & Böttcher, 2014, JHEAp)

Distinguishing Diagnostic: Variability

- Time-dependent hadronic models can produce uncorrelated variability / orphan flares

(Dimitrakoudis et al. 2012, Mastichiadis et al. 2013, Weidinger & Spanier 2013, Diltz et al. 2015)

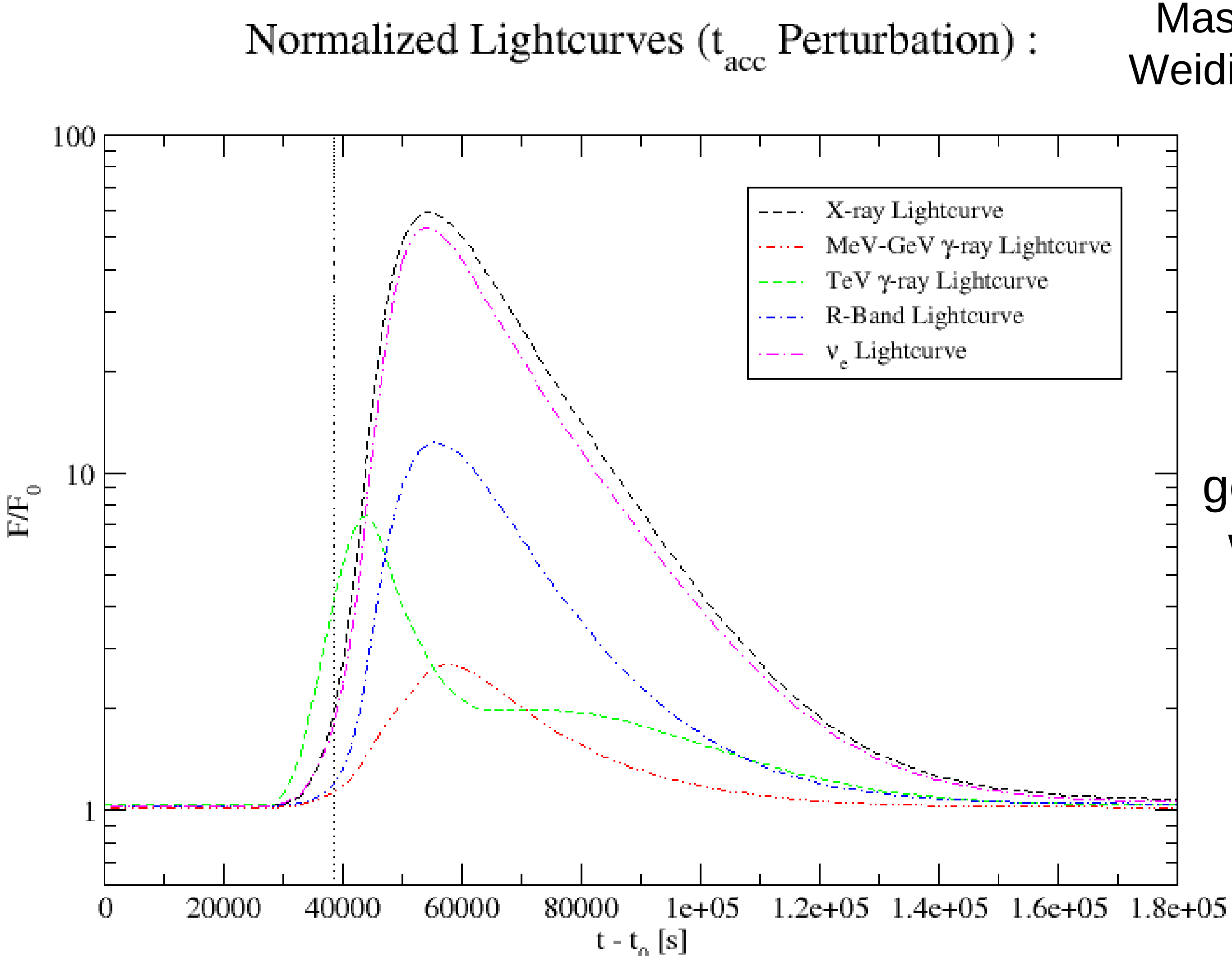

Neutrino flares generally co-incident with X-ray through GeV γ-ray flares

(Diltz et al. 2015)

Total Energy Loss Rate of Relativistic Electrons

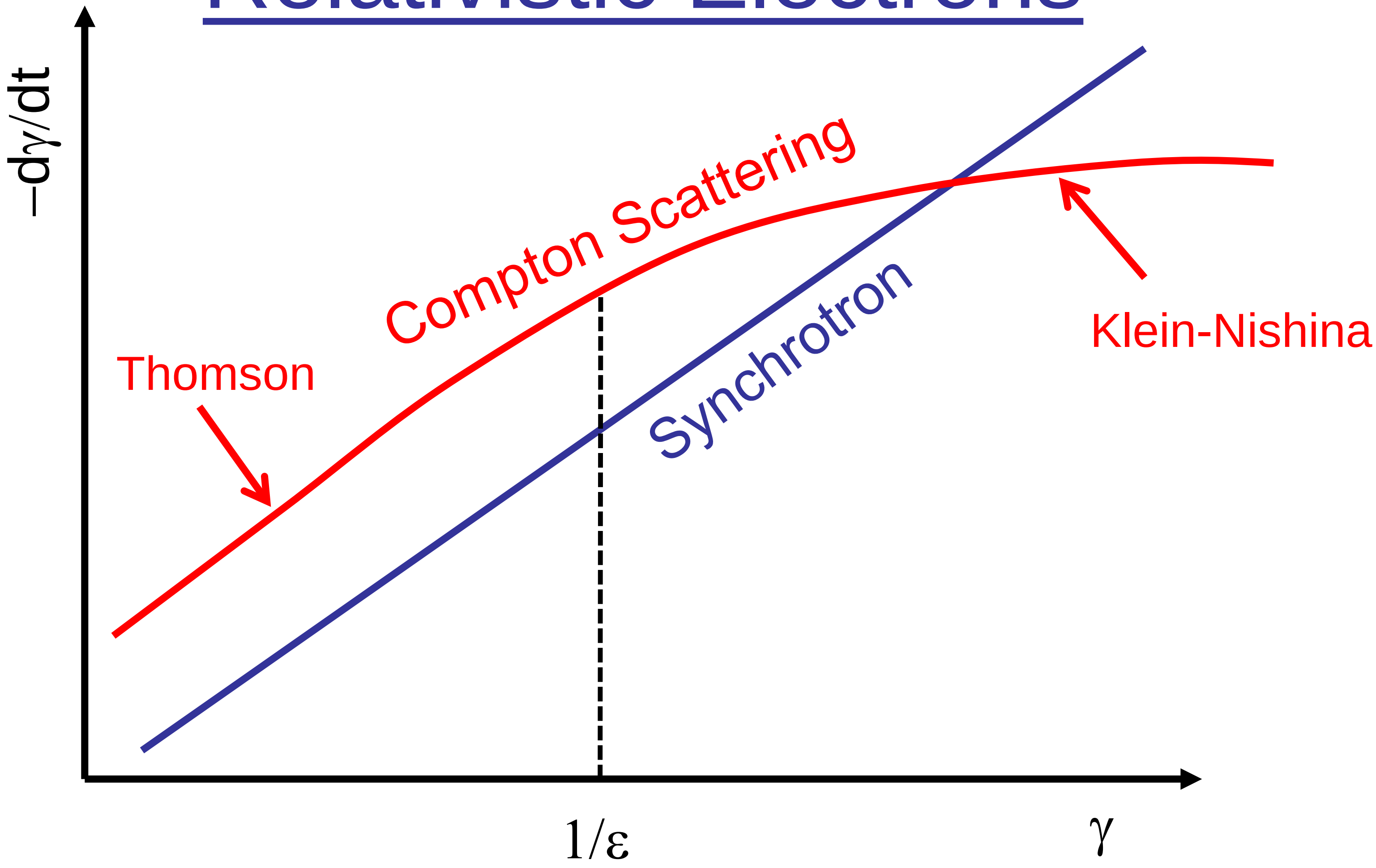

Compton energy loss becomes less efficient at high energies (Klein-Nishina regime).

Diagnosing the Location of the Blazar Zone

FSRQs: Electron cooling dominated by Compton scattering

If seed photons are from IR torus: $\rightarrow$ Thomson $\rightarrow \gamma \sim \gamma^2$
$\rightarrow t_{cool} \sim \gamma^{-1}$

If seed photons are from BLR (optical/UV):
$\rightarrow$ Klein-Nishina $\rightarrow \gamma \sim \gamma^{\alpha}$
$\alpha < 2$
$\rightarrow t_{cool} \sim$ const.

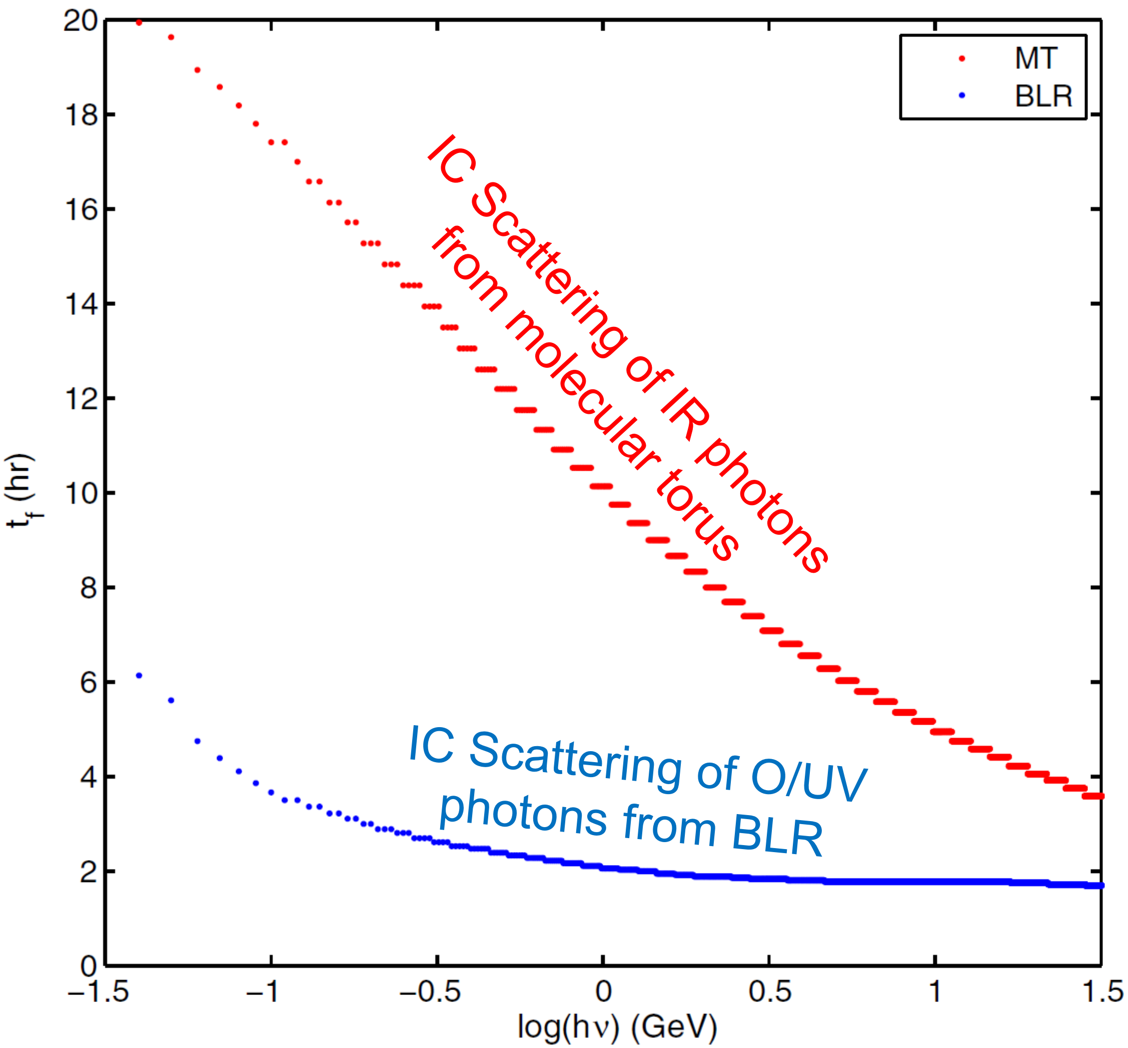

(Dotson et al. 2012)

Calculation of X-Ray and Gamma-Ray Polarization in Leptonic and Hadronic Blazar Models

- Synchrotron polarization:

  Standard Rybicki & Lightman description

- SSC Polarization:

  Bonometto & Saggion (1974) for Compton scattering in Thomson regime

- External-Compton emission: Unpolarized.

Upper limits on high-energy polarization, assuming perfectly ordered magnetic field perpendicular to the line of sight (Zhang & Böttcher 2013)